

# Mechanics of the Respiratory Muscles

André De Troyer<sup>\*1</sup> and Aladin M. Boriek<sup>2</sup>

## ABSTRACT:

This article examines the mechanics of the muscles that drive expansion or contraction of the chest wall during breathing. The diaphragm is the main inspiratory muscle. When its muscle fibers are activated in isolation, they shorten, the dome of the diaphragm descends, pleural pressure ( $P_{pl}$ ) falls, and abdominal pressure ( $P_{ab}$ ) rises. As a result, the ventral abdominal wall expands, but a large fraction of the rib cage contracts. Expansion of the rib cage during inspiration is produced by the external intercostals in the dorsal portion of the rostral interspaces, the intercartilaginous portion of the internal intercostals (the so-called parasternal intercostals), and, in humans, the scalenes. By elevating the ribs and causing an additional fall in  $P_{pl}$ , these muscles not only help the diaphragm expand the chest wall and the lung, but they also increase the load on the diaphragm and reduce the shortening of the diaphragmatic muscle fibers. The capacity of the diaphragm to generate pressure is therefore enhanced. In contrast, during expiratory efforts, activation of the abdominal muscles produces a rise in  $P_{ab}$  that leads to a cranial displacement of the diaphragm into the pleural cavity and a rise in  $P_{pl}$ . Concomitant activation of the internal interosseous intercostals in the caudal interspaces and the triangularis sterni during such efforts contracts the rib cage and helps the abdominal muscles deflate the lung. © 2011 American Physiological Society. *Compr Physiol* 1:1273-1300, 2011.

## Introduction

The respiratory muscles are those skeletal muscles that drive expansion or contraction of the chest wall during breathing and, thus, pump air in and out of the lungs. Because the mechanics of a skeletal muscle is essentially determined by the anatomy of the muscle and by the structures it displaces when it contracts, the present article starts with a discussion of the basic mechanical structure of the chest wall. It next analyzes the mechanics of each group of muscles. For the sake of clarity, the mechanics of the diaphragm, the intercostal muscles, the muscles of the neck, and the muscles of the abdominal wall are analyzed sequentially. However, since all these muscles work together in a coordinated manner during breathing, the mechanical interactions between them are also examined. To be sure, many of these muscles are also involved in a variety of nonrespiratory activities, such as vomiting, defecation, and trunk motion, but these functions are not covered in this review.

## The Chest Wall

The chest wall can be thought of as consisting of two compartments—the rib cage and the abdomen—separated by a thin musculotendinous structure, the diaphragm (99) (Fig. 1). These two compartments are mechanically arranged in parallel. Expansion of the lungs, therefore, can be accomplished by expansion of either the rib cage or the abdomen or of both compartments simultaneously.

The displacements of the rib cage during breathing are essentially related to the motion of the ribs. Each rib articulates

at its head with the bodies of its own vertebra and of the vertebra above, and at its tubercle with the transverse process of its own vertebra. The head of the rib is closely connected to the vertebral bodies by radiate and intra-articular ligaments, such that only slight gliding movements of the articular surfaces can occur. Also, the neck and tubercle of the rib are bound to the transverse process of the vertebra by short ligaments that limit the movements of the costovertebral joint to slight cranial and caudal gliding. Thus the costovertebral and costovertebral joints together form a hinge, and the displacements of the rib during breathing occur primarily through a rotation around the long axis of its neck, as shown in Figure 2 A. This axis is oriented laterally, dorsally, and caudally. In addition, the ribs are curved and slope caudally and ventrally from their costovertebral articulations, such that their ventral ends, the costal cartilages, and the junctions of the cartilages with the sternum are more caudal than their dorsal part (Fig. 2, B and C). When the ribs are displaced in the cranial direction, therefore, their ventral ends move laterally and ventrally as well as cranially, the costal cartilages rotate cranially around the chondrosternal junctions, and the sternum is displaced ventrally. As a result, both the lateral and the dorsoventral diameters of the rib cage usually increase (Fig. 2, B and C); the

\*Correspondence to a.detroyer@yahoo.fr

<sup>1</sup>Chest Service, Erasme University Hospital, and Laboratory of Cardiorespiratory Physiology, Brussels School of Medicine, Brussels, Belgium

<sup>2</sup>Department of Medicine, Baylor College of Medicine, Houston, Texas

Published online, July 2011 ([comprehensivephysiology.com](http://comprehensivephysiology.com))

DOI: 10.1002/cphy.c100009

Copyright © American Physiological Society

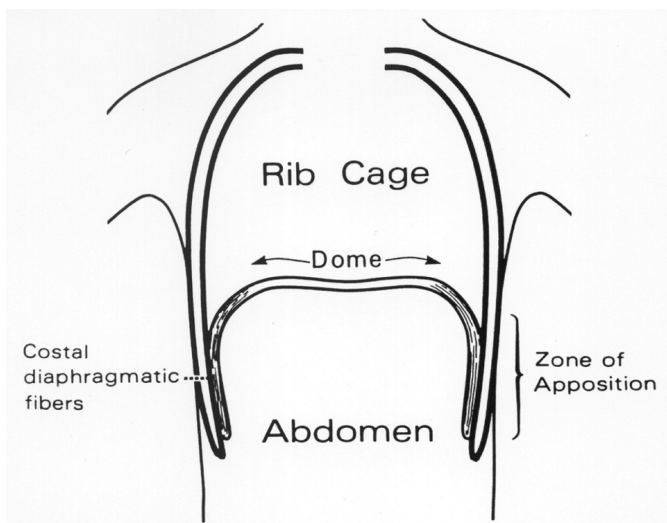


**Figure 1** Coronal section of the human chest wall at end expiration. The costal diaphragmatic fibers run mainly cranially from their insertions on the lower ribs and are directly apposed to the inner aspect of the lower rib cage (zone of apposition). (Reproduced, with permission, from De Troyer A, Loring SH. *Actions of the respiratory muscles*. In: Roussos C, editor. *The Thorax* (2nd ed), Vol. 85. New York: Marcel Dekker, 1995, pp. 535-563).

component of rib rotation that occurs around the transverse axis is conventionally called the “pump-handle” component, and the component that occurs around the dorsoventral axis is conventionally called the “bucket-handle” component. Conversely, a caudal displacement of the ribs is usually associated with a decrease in the lateral and the dorsoventral diameters of the rib cage. This pattern of rib motion implies that the muscles that elevate the ribs have an inspiratory effect on the rib cage, whereas the muscles that lower the ribs have an expiratory effect.

It is notable, however, that although all the ribs move predominantly by a rotation around the axis of their neck, the costovertebral joints of ribs 7 to 10 have less constraint on their motion than the costovertebral joints of ribs 1 to 6. Also, whereas the ribs 1 to 6 are connected to the sternum by short costal cartilages, ribs 8 to 10 have long costal cartilages that articulate with one another by little synovial cavities. Hence, the upper ribs tend to move as a unit with the sternum, but the lower ribs have greater freedom of motion. Both in animals and in humans, deformations of the rib cage may therefore occur during contraction of the muscles that insert on it.

The respiratory displacements of the abdominal compartment are more straightforward than those of the rib cage because if one neglects the 100 to 300 ml of abdominal gas volume, its contents are virtually incompressible. This implies that any inward displacement of parts of the surrounding container results in an equal outward displacement of other parts. Furthermore, many of these boundaries, such as the spine dorsally, the pelvis caudally, and the iliac crests laterally, are virtually fixed. Consequently, the parts of the abdominal

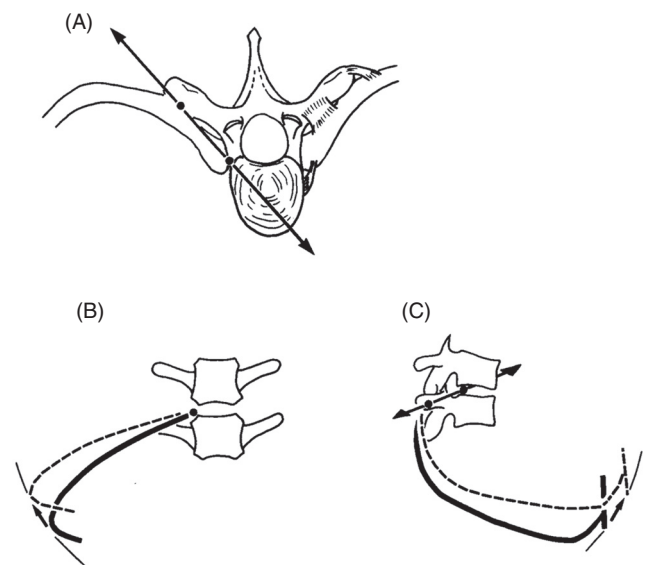


**Figure 2** Respiratory displacements of the rib cage. (A) diagram of a typical thoracic vertebra and a pair of ribs (viewed from above). Each rib articulates with both the body and the transverse process of the vertebra (closed circles) and is bound to it by strong ligaments (right). The motion of the rib, therefore, occurs primarily through a rotation around the axis defined by these articulations (solid line and double arrow-head). (B) and (C) ventral and lateral views, respectively, of the rib at end expiration (solid lines) and end inspiration (dotted lines). When the rib becomes more horizontal in inspiration, the transverse (B) and the anteroposterior (C) diameter of the rib cage increase (small arrows), and the sternum is displaced ventrally (vertical line in C). (Reproduced, with permission, from De Troyer A. *Respiratory muscle function*. In: Shoemaker WC, Ayres SM, Grenvik A, Holbrook PR, editors. *Textbook of Critical Care*. W.B. Saunders, 2000, pp. 1172-1184).

container that can be displaced are largely limited to the ventral abdominal wall and the diaphragm. When the diaphragm descends (see below), therefore, abdominal pressure ( $P_{ab}$ ) increases, and the ventral wall of the abdomen is displaced outward; conversely, when the abdominal muscles contract, the ventral abdominal wall moves inward,  $P_{ab}$  rises, and the diaphragm is displaced cranially into the thoracic cavity.

## The Diaphragm

### Functional anatomy

The muscle fibers of the diaphragm radiate from a central tendinous structure, the “central tendon,” to insert peripherally into skeletal structures. Depending on the nature of these skeletal structures, the muscle of the diaphragm is conventionally divided into two main components: (i) the crural (or vertebral) portion that, in humans, inserts on the ventrolateral aspect of the first three lumbar vertebrae and on the aponeurotic arcuate ligaments; and (ii) the costal portion that inserts on the xiphoid process of the sternum and the upper margins of the lower six ribs. When projected on a lateral view of the thorax, the line of insertion of the diaphragm on the ribs slants

caudally and dorsally, and the muscle fibers of the costal portion run nearly perpendicular to this line of insertion (11). From their insertions on the ribs, therefore, the costal muscle fibers run obliquely in the cranial-dorsal direction. Although the older literature suggested the possibility of an intercostal motor innervation of some portions of the diaphragm (145), it is now clearly established that the only motor supply to the muscle is through the phrenic nerves. Thus, both in humans and in the dog, each phrenic nerve supplies its own hemidiaphragm, including all the fibers in the crural portion on its own side of the esophageal hiatus (13, 102), and when a phrenic nerve is sectioned, the corresponding hemidiaphragm is paralyzed and undergoes atrophy (13, 94, 153).

Because the muscle fibers of the costal diaphragm run in the cranial-dorsal direction from their insertions on the ribs, they are directly apposed to the inner aspect of the lower rib cage and constitute the so-called “zone of apposition” of the diaphragm to the rib cage, as shown in Figure 1 (129). In humans at FRC (functional residual capacity), this zone of apposition represents approximately 25% to 40% of the total surface area of the rib cage (130) and approximately 60% to 65% of the total surface area of the muscle (82, 139). The result of this anatomic arrangement is that the diaphragm is usually regarded as an elliptical cylindroid capped by a dome, the cylindrical part corresponding to the zone of apposition and the dome being primarily made of the central tendon.

As the muscle fibers of the diaphragm are activated during inspiration, they develop tension and shorten. As a result, the axial length of the apposed diaphragm diminishes and the dome of the diaphragm descends relative to its costal insertions. The central tendon is very stiff and effectively inextensible (93), so the dome of the diaphragm remains essentially constant in size as it descends. A remarkable feature of the diaphragm, however, is that the shape of the muscular portion is also relatively constant, independent of the differences in muscle tension that may occur. Specifically, using biplane fluoroscopy to measure the curvatures of the mid-costal diaphragm in supine dogs, Boriek et al. (9) showed that the curvatures both in the direction of the muscle fibers and in the direction perpendicular to the muscle fibers at end-inspiration were similar to those at the relaxed FRC and to those after passive inflation as well. The curvature of the muscle was also nearly constant after the animals were shifted from the supine to the prone posture. The mechanism that allows the diaphragm to maintain such a stable shape remains uncertain, but a finite element model analysis has suggested that the inextensibility of the central tendon and the anisotropy of the muscular portion play a major role in this phenomenon (10). Indeed, stretch experiments of canine diaphragm strips *in vitro* have shown that the stiffness of the muscle in the direction transverse to the muscle fibers is substantially greater than that along the muscle fibers (8, 93). It should be pointed out, however, that, although the muscle is stiffer in the direction transverse to the muscle fibers, this stiffness is not high enough to account for the observation that during diaphragmatic contraction, strain in the transverse direction is very

small. Based on this observation, one can therefore infer that during contraction, stress is small in the direction transverse to the muscle fibers and significant only along the muscle fibers (7, 8).

## Respiratory action of the diaphragm

During breathing, therefore, the diaphragm functions essentially like a piston, and the descent of the dome produces both an expansion of the pleural cavity along its craniocaudal axis and a caudal displacement of the abdominal viscera leading to an outward motion of the ventral abdominal wall. Consequently, intrapleural pressure ( $P_{pl}$ ) falls and, if the airway is open, lung volume increases. Moreover,  $P_{ab}$  rises, and at equilibrium, the force generated by the active diaphragm balances the difference between  $P_{ab}$  and  $P_{pl}$ , that is, transdiaphragmatic pressure ( $P_{di}$ ).

In addition, measurements of thoracoabdominal motion in subjects with complete, traumatic transection of the lower cervical cord, in whom the diaphragm is the only muscle active during resting inspiration, have shown that in humans, the diaphragm contracting alone also displaces the rib cage. Thus, when such subjects are breathing at rest in the seated posture, they have an inspiratory decrease in the anteroposterior diameter of the upper rib cage together with an increase in the diameters, particularly the transverse diameter, of the lower rib cage (69, 133). Measurements of thoracoabdominal motion during phrenic nerve pacing in subjects with transection of the upper cervical cord have confirmed that the isolated diaphragm in humans has an expiratory action on the upper rib cage and an inspiratory action on the lower rib cage (22, 154).

### Mechanisms of action of the diaphragm on the rib cage

The inspiratory action of the diaphragm on the lower rib cage is, in part, related to the insertions of the muscle on the lower ribs. Thus, because the muscle fibers run mainly cranially from their insertions on the lower ribs, they exert a cranially oriented force on these ribs when they contract. This force, conventionally referred to as the “insertional force,” has therefore the effect of lifting the lower ribs and rotating them outward (60, 120). Moreover, the existence of a zone of apposition of the diaphragm to the rib cage (Fig. 1) makes the lower rib cage, in effect, part of the abdominal container, and measurements in dogs have shown that, during resting breathing, the changes in pressure in the pleural recess between the apposed diaphragm and the rib cage are nearly equal to the changes in  $P_{ab}$  (157). Pressure in this pleural recess rises, rather than falls, during inspiration, thus indicating that the rise in  $P_{ab}$  is truly transmitted through the apposed diaphragm to expand the lower rib cage. The force thus developed by the diaphragm on the lower rib cage through the rise in  $P_{ab}$  has been called the “appositional” force (60, 120), and its magnitude depends, in part, on the size of the zone of

apposition. Both in humans (69, 82) and in the dog (11), the area of apposed diaphragm at the lateral rib cage is greater than that at the ventral rib cage, and this probably accounts for the fact that isolated contraction of the diaphragm in humans expands the lower rib cage more along its transverse than its anteroposterior diameter (69).

The respective roles played by the insertional and appositional forces in determining the inspiratory action of the diaphragm on the lower rib cage have not been assessed. It should be appreciated, however, that these forces are largely determined by the elastance of the abdomen. If abdominal elastance is increased (i.e., if abdominal compliance is decreased), the descent of the dome of the diaphragm in response to a given muscle activation is smaller, the zone of apposition at end-inspiration is larger, and the rise in  $P_{ab}$  is greater. Therefore, the appositional and insertional forces are increased. A dramatic illustration of this phenomenon is provided by quadriplegic subjects given an external abdominal compression; in such subjects, when a passive mechanical support to the abdomen is provided by a pneumatic cuff or an elastic binder, the expansion of the lower rib cage during inspiration is larger (22, 154). Conversely, if abdominal elastance is reduced (i.e., if the abdomen is more compliant), the dome of the diaphragm descends more easily, the zone of apposition at end-inspiration is smaller, and the rise in  $P_{ab}$  is also smaller. Consequently, the inspiratory expansion of the lower rib cage is decreased. Such a decrease in abdominal elastance occurs when humans change from the seated to the supine posture (71, 149), and indeed, whereas the contracting diaphragm in seated quadriplegic subjects causes an increase in the anteroposterior diameter of the lower rib cage, in the supine posture, it produces a decrease in this diameter (22, 69, 154); in such subjects, the increase in the transverse diameter of the lower rib cage during inspiration is also less in the supine than in the seated posture (69).

On the other hand, isolated contraction of the diaphragm in quadriplegic subjects causes a decrease in the anteroposterior diameter of the upper rib cage in all body positions. Similarly, when the diaphragm in anesthetized dogs and rabbits is activated selectively by electrical stimulation of the phrenic nerves, the upper ribs move caudally and the transverse diameter of the upper rib cage decreases. When the stimulation of the phrenic nerves is then repeated after bilateral pneumothoraces have been introduced so as to uncouple the rib cage from the lung and eliminate the fall in  $P_{pl}$ , however, the upper ribs remain stationary and the transverse diameter of the upper rib cage is unaltered (26, 50). These observations indicate that the effect on the upper ribs of the insertional and appositional forces developed by the diaphragm is relatively small and that the action of the muscle on these ribs is primarily the result of the fall in  $P_{pl}$ .

### Response to phrenic nerve stimulation

Whereas the respiratory action of the diaphragm in humans has been primarily inferred from observations obtained dur-

ing breathing in subjects with quadriplegia, studies of the action of the muscle in animals have been performed using isolated supramaximal stimulation of the phrenic nerves. This technique is useful to study the mechanics of the diaphragm, because it produces a constant, well-defined level of muscle activation and avoids simultaneous contraction of other muscles. Therefore, it allows accurate assessments of the relationships among muscle length, muscle displacement,  $\Delta P_{pl}$ , and  $\Delta P_{ab}$  to be made. It also allows for the precise evaluation of the response of the diaphragm to different conditions, such as lung inflation and ascites (see below). Isolated stimulation of the phrenic nerves, however, produces extreme shortening of the muscle fibers and marked distortion of the rib cage. Specifically, in anesthetized dogs, whereas the diaphragm shortens by 5% to 10% of its resting, end-expiratory length during quiet inspiration (12, 68, 134, 151), during isolated supramaximal phrenic nerve stimulation at FRC, the muscle shortens by approximately 40% (6, 51, 68, 89). In this condition, therefore, the zone of apposition decreases markedly, so that most of the lower rib cage becomes exposed to the expiratory effect of  $P_{pl}$ , rather than the inspiratory effect of  $P_{ab}$ . As a result, the lowermost ribs also move caudally, rather than cranially (51).

As Leduc et al. (104) have pointed out, however, the change in length of the costal portion of the diaphragm in a given maneuver is, as a first approximation, proportional to the relative displacement of the dome and the muscle insertions into the lower ribs. It would be expected, therefore, that a given diaphragm shortening would produce a larger descent of the dome if the muscle insertions into the ribs move caudally than it would if these insertions did not move. Using computed tomography, De Troyer et al. (51) recently measured diaphragm length and displacement in dogs to evaluate the role played by the caudal motion of the lower ribs in producing the descent of the dome of the diaphragm during isolated, supramaximal phrenic stimulation, and they concluded that in this condition, the caudal motion of the lower ribs contributes nearly a quarter of the descent of the dome. In addition, based on the fact that the descent of the dome is the primary cause of  $\Delta P_{pl}$  during isolated diaphragm contraction, these investigators further speculated that the caudal motion of the lower ribs, taken alone, would make a significant contribution to the total  $\Delta P_{pl}$  generated by the diaphragm. This hypothesis, however, remains to be validated.

### Effect of lung inflation

It has long been recognized that, when the airways in dogs (97, 124, 132), cats (72, 124, 137), and rabbits (146) are occluded and the diaphragm is selectively activated by stimulation of the phrenic nerves, the  $\Delta P_{pl}$  or  $\Delta P_{ao}$  that occurs during stimulation is closely dependent on the lung volume before stimulation. Data obtained in a recent study in six dogs (51) are shown in Figure 3. When phrenic nerve stimulation was performed at FRC,  $\Delta P_{ao}$  was  $-34.8 \pm 2.8$  cmH<sub>2</sub>O. However, this pressure change decreased rapidly and continuously as lung volume increased, such that, when phrenic nerve stimulation

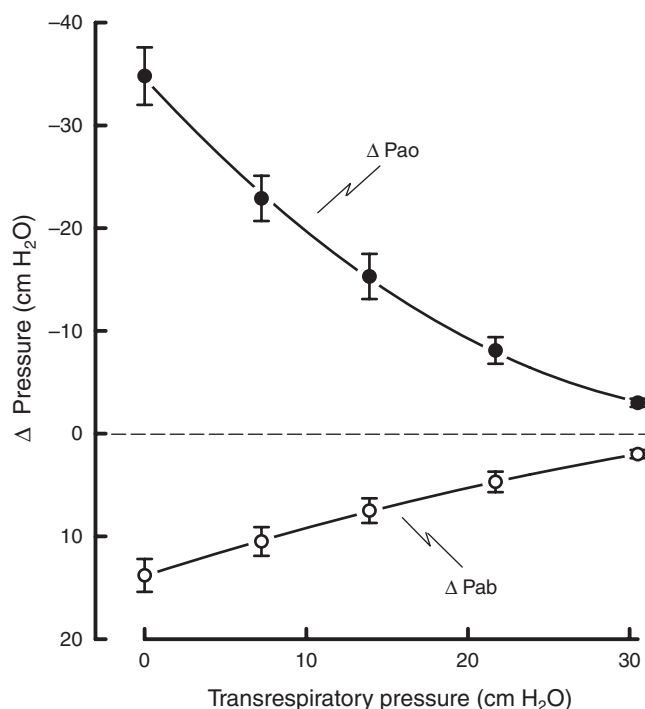


**Figure 3** Mean  $\pm$  SE changes in airway opening pressure ( $\Delta P_{ao}$ ) and abdominal pressure ( $\Delta P_{ab}$ ) obtained from six dogs during isolated, bilateral stimulation of the phrenic nerves at five different lung volumes from FRC (transrespiratory pressure = 0 cmH<sub>2</sub>O) to TLC (transrespiratory pressure = 30 cmH<sub>2</sub>O). All stimulations were performed while the endotracheal tube was occluded. The capacity of the diaphragm to generate pressure, in particular pleural pressure, decreases markedly with increasing lung volume. (Reproduced, with permission, from ref. 51).

was performed at TLC (total lung capacity) (transrespiratory pressure = 30 cmH<sub>2</sub>O), it was only  $-3.0 \pm 0.4$  cmH<sub>2</sub>O. The rise in  $P_{ab}$  during stimulation also decreased progressively as lung volume increased from FRC ( $13.8 \pm 1.6$  cmH<sub>2</sub>O) to TLC ( $2.3 \pm 0.4$  cmH<sub>2</sub>O). A similar decline in  $\Delta P_{pl}$  with increasing lung volume has been reported by Danon et al. (22) in three subjects with transection of the upper cervical cord and phrenic nerve pacing, and by Smith and Bellemare (150) in six healthy individuals during stimulation of the phrenic nerves with single twitches. Thus, both in animals and in humans, the capacity of the diaphragm to generate pressure, in particular  $P_{pl}$ , decreases with increasing lung volume and is almost zero at TLC. The primary cause of this lung volume dependence lies in the relation between the contractile force developed by the muscle and its length.

### Force-length relationship of the diaphragm

As reviewed in detail in the previous article of this Handbook (Reid & Sieck) in *Comprehensive Physiology*, the force developed by a skeletal muscle bundle during isometric contraction *in vitro* varies with the length of the muscle. Specifically, as the length of the muscle during contraction increases, active force increases until a maximum is reached. The length cor-

responding to the maximum active force is usually referred to as the optimal length ( $L_o$ ), and when muscle length increases beyond  $L_o$ , active force decreases again. McCully and Faulkner (126) studied the force-length relationship in excised diaphragmatic muscle bundles from five animal species (rats, cats, dogs, pigs, and monkeys), and they demonstrated that the relationship for the diaphragm is essentially similar to that for limb muscles.

To assess the force-length relationship for the diaphragm *in vivo*, Road et al. (142) measured diaphragm muscle length (by sonomicrometry) and  $P_{ab}$  in supine dogs while supra-maximal stimuli were delivered to the phrenic nerves in the thorax. As the animals had bilateral pneumothoraces,  $P_{pl}$  was zero and  $\Delta P_{ab}$  reflected muscle force. Also, the abdomen and lower rib cage in the preparation were enclosed in a cast, and diaphragm length was controlled by a piston that penetrated the cast. As is shown in Figure 4, the relationship between  $P_{di}$  and muscle length in these animals (dashed line) was similar to the force-length curve obtained for diaphragmatic muscle bundles *in vitro* (75, 126). Thus  $P_{di}$  was greatest when muscle length during stimulation was near the relaxed FRC length ( $L_{FRC}$ ), and it decreased progressively as muscle length decreased such that it was approximately zero when muscle length was approximately 40% of  $L_{FRC}$ . Road et al. (142) concluded, therefore, that in supine dogs, the relaxed diaphragm at FRC is close to  $L_o$ ; several studies comparing diaphragm muscle length in supine dogs with  $L_o$  measured *in vitro* have amply confirmed this conclusion (75, 76, 122). In addition, Road et al. (142) also concluded that  $P_{di}$  is primarily or exclusively determined by the length of the diaphragm during contraction, thus suggesting that the adverse effect of lung inflation on  $P_{di}$  would be the result of the decrease in active muscle length.

The role of diaphragm muscle length in determining the lung-volume dependence of  $P_{di}$  was subsequently examined by Hubmayr et al. (89) and De Troyer et al. (51). Using biplane fluoroscopy or computed tomography, these investigators measured diaphragm muscle length in dogs while the phrenic nerves were stimulated in the neck at different lung volumes. In contrast to Road et al. (142), the pleural space in these animals was left intact (so  $P_{di} = P_{ab} - P_{pl}$ ). In addition, and more importantly, the abdomen and rib cage were not constrained, so that the diaphragm was allowed to shorten substantially during phrenic nerve stimulation. The two studies reported essentially similar results. In the study by De Troyer et al. (51) for example, during stimulation at FRC, the muscle shortened to 60% of  $L_{FRC}$ , and  $P_{di}$  was, on average,  $54.5 \pm 3.7$  cmH<sub>2</sub>O. As shown in Figure 4, therefore, the data point corresponding to FRC was very close to the curve obtained by Road et al. (142). As lung volume increased from FRC, however,  $P_{di}$  during stimulation decreased markedly, but diaphragm muscle length decreased only moderately; at TLC,  $P_{di}$  was  $5.3 \pm 0.8$  cmH<sub>2</sub>O while muscle length was 51% of  $L_{FRC}$ . Consequently, the data points corresponding to higher lung volumes lay well below the curve obtained by Road et al. (142) (Fig. 4). In other words, during

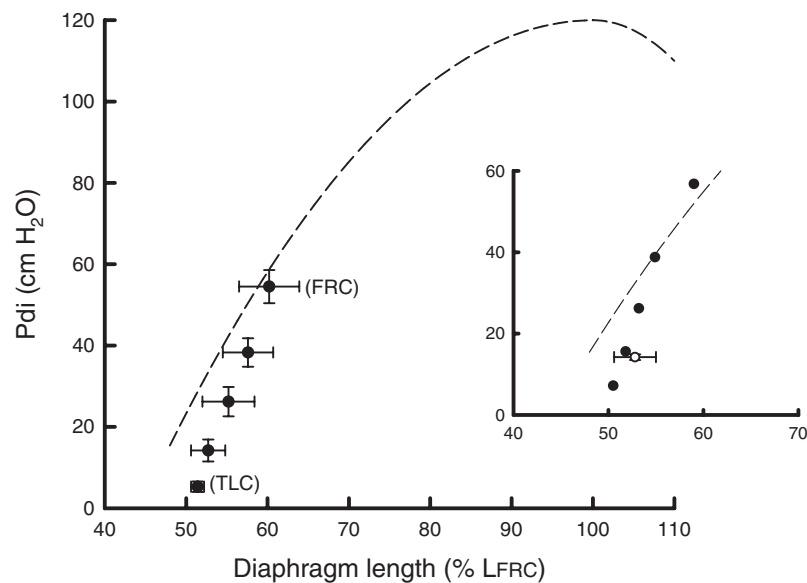


**Figure 4** Relationship between transdiaphragmatic pressure ( $P_{di}$ ) and diaphragm muscle length during isolated, supramaximal phrenic nerve stimulation at different lung volumes. The dashed line in the main panel is the aggregate relationship obtained for the costal and crural portions of the canine diaphragm *in vivo* by Road et al. (136), and the closed circles are the mean  $\pm$  SE values obtained from six dogs (same animals as in Figure 3) during phrenic nerve stimulation at increasing lung volumes from FRC (top circle) to TLC (bottom circle). Muscle length was measured by computed tomography and is expressed as a percentage of muscle length during relaxation at FRC ( $L_{FRC}$ ). Note that the data point obtained at FRC is close to the length-tension relationship of Road et al., but the data points obtained at high lung volumes lay well below the curve. Data in the inset are the mean values obtained before (closed circles) and after (open circle; bars,  $\pm$  SE) bilateral pneumothorax in a subset of four animals. (Redrawn, with permission, from ref. 63).

isolated phrenic nerve stimulation at high lung volumes,  $P_{di}$  was smaller than anticipated on the basis of muscle length alone.

Because the abdominal contents are incompressible, the changes in  $P_{ab}$  during slow breathing maneuvers and expulsive efforts are essentially uniform throughout the abdominal cavity (131). On the other hand, measurements of pleural surface pressure in dogs have shown that significant topographic differences in  $\Delta P_{pl}$  may occur during breathing depending on the pattern of respiratory muscle contraction (27). Specifically, after the phrenic nerves in the animals were sectioned, so that breathing was entirely accomplished by the inspiratory intercostal muscles, the values of  $\Delta P_{pl}$  over the apex of the lung were larger than those over the lung base. Conversely, during isolated stimulation of the phrenic nerves, the values of  $\Delta P_{pl}$  over the base of the lung were larger. To the extent that the values of  $\Delta P_{pl}$  reported by Hubmayr et al. (89) and De Troyer et al. (51) were obtained, respectively, with a balloon-catheter system placed in the esophagus and a catheter connected to the endotracheal tube, the possibility therefore had to be considered that these values were smaller than the pressure changes over the lung-apposed surface of the diaphragm, and, hence, that the values of  $P_{di}$  in these studies underestimated the actual pressure differences across the diaphragm.

This possibility was tested experimentally in four of the six dogs reported in Figures 3 and 4. Thus, after the phrenic nerves were stimulated at different lung volumes, bilateral pneumothoraces were performed so as to abolish the topographic differences in  $\Delta P_{pl}$ , and stimulation of the phrenic nerves was repeated (unpublished observations). The results of this experiment are shown in the inset of Figure 4. Muscle length during phrenic stimulation after pneumothorax was 52.8% of  $L_{FRC}$ , and  $P_{di}$  was 14.2 cmH<sub>2</sub>O. As a result, the data point (open circle) was very close to that obtained in the intact animals after passive lung inflation to a transrespiratory pressure of +21 cmH<sub>2</sub>O, that is, it remained well below the curve obtained by Road et al. (142). It follows from this observation that in supine dogs, a factor other than muscle length operates to reduce  $P_{di}$  during phrenic stimulation at high lung volumes.

The diaphragm is sufficiently thin so that it can be regarded as a membrane, and the pressure difference across a membrane is proportional both to the membrane stress and to the curvature (Laplace's law). In an attempt to explain the marked decrease in  $P_{di}$  during isolated phrenic nerve stimulation at high lung volumes, Boriek et al. (6, 12) therefore measured both the changes in length and the changes in curvature of the canine diaphragm during spontaneous inspiratory efforts and during isolated phrenic nerve stimulation at different lung volumes. When the animals performed spontaneous

inspiratory efforts at lung volumes between FRC and TLC, muscle length decreased to 85% to 60% of  $L_{FRC}$ , and the radius of muscle curvature remained nearly constant. However, when the phrenic nerves were stimulated, muscle length decreased further to 50% to 60% of  $L_{FRC}$ , and the radius of diaphragm curvature increased sharply (6). In agreement with this finding, De Troyer and Wilson (63) observed that as diaphragm muscle length during phrenic stimulation decreased from 60%  $L_{FRC}$  at FRC to 51%  $L_{FRC}$  at TLC (Fig. 4), the radius of curvature of the mid-costal diaphragm increased by a factor of two. Thus, with isolated maximal diaphragm activation in the intact animal, the curvature of the muscle decreases as muscle length decreases, and this decrease in curvature adds to the decrease in muscle length to reduce  $P_{di}$  at high lung volumes.

The question arises, therefore, as to what causes diaphragm muscle length to be smaller during maximal activation at TLC than during maximal activation at FRC. The answer to the question lies in the difference in the load imposed on the muscle by the lung and chest wall. Thus, as we have previously pointed out, when the diaphragm is activated, the muscle fibers shorten, the dome of the diaphragm descends,  $P_{pl}$  decreases, and  $P_{ab}$  increases, and at equilibrium, the  $P_{di}$  generated by the muscle balances the load imposed by  $P_{pl}$  and  $P_{ab}$ . The interplay between the pressure generated by the muscle, the load applied to the muscle, and muscle length can be illustrated by using the diagram shown in Figure 5 (63, 162).

### Graphical representation of diaphragm action

The continuous lines in this diagram are the  $P_{di}$ -length relationships obtained for the maximally active and the passive diaphragm in supine dogs: muscle length is expressed as a fraction of  $L_o$  (or  $L_{FRC}$ ), and  $P_{di}$  is expressed as a fraction of the value during maximal activation at  $L_o$  (maximal value). As we discussed earlier,  $P_{di}$  during supramaximal phrenic nerve stimulation decreases gradually as muscle length decreases from  $L_{FRC}$  to 60% of  $L_{FRC}$ , and it then decreases more rapidly as muscle length decreases further to approximately 50% of  $L_{FRC}$ . Also, measurements of diaphragm muscle length (51, 152, 158) and  $P_{di}$  (48, 89, 137, 142) have established that, during relaxation in supine dogs and cats, the action of gravity on the abdominal visceral mass induces stretching of the diaphragm and, therefore, elicits a significant amount of passive tension (and  $P_{di}$ ) in the muscle at FRC. During passive inflation, however, the rise in  $P_{pl}$  reduces the load on the diaphragm. As a result, the dome of the diaphragm descends, muscle length decreases, and passive tension decreases as well. Passive  $P_{di}$ , in fact, is essentially eliminated at a muscle length corresponding to approximately 70% of  $L_{FRC}$ .

The dashed lines in Figure 5 represent the load imposed on the diaphragm by  $P_{di}$  as a function of diaphragm length at FRC and at TLC, and they are drawn so that the load line at each lung volume intersects the maximally active  $P_{di}$ -length curve at the observed values of muscle length and  $P_{di}$ . At FRC,

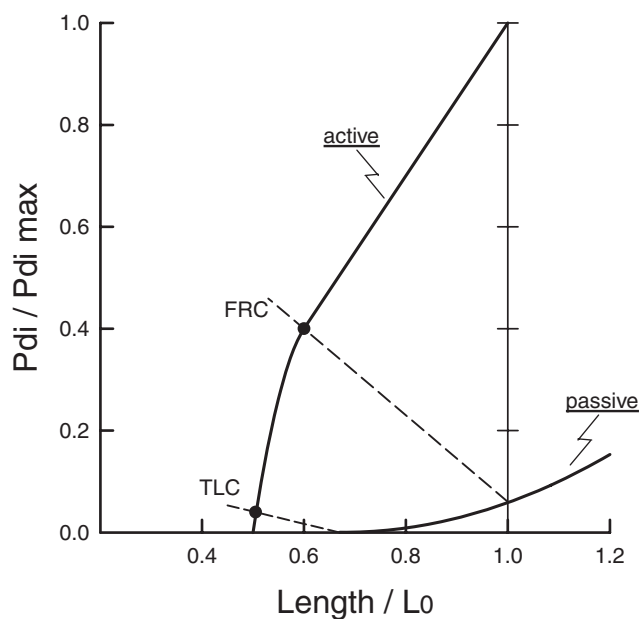


**Figure 5** Graphical representation of the effect of inflation on the pressure developed by the diaphragm. The continuous lines are the  $P_{di}$ -length relationships for the maximally active and the passive diaphragm, and the dashed lines are the load lines describing the load imposed by the lung and chest wall on the diaphragm during isolated contraction at FRC and during isolated contraction at TLC.  $P_{di}$  is expressed as a fraction of the maximal value, and muscle length is expressed as a fraction of optimal length ( $L_o$ ). The pressure developed by the diaphragm during phrenic nerve stimulation at a given lung volume is given by the intersection (closed circle) of the load line with the maximally active  $P_{di}$ -length curve. (Reproduced, with permission, from ref. 63).

the relaxed diaphragm is close to  $L_o$ , and when the muscle is maximally activated against an occluded airway, it shortens to approximately 60% of  $L_o$  so that  $P_{di}$  is approximately 0.40 of its maximal value. With passive inflation from FRC to TLC, however, the decrease in the load on the relaxed diaphragm causes the muscle to shorten to approximately 70% of  $L_{FRC}$  (51, 75, 134, 152, 158). In addition, it is well established that the elastance of the rib cage in dogs is larger at low lung volumes and decreases as lung volume increases (26, 37). Therefore, compared with the load line at FRC, the load line for TLC is displaced downward and is not as steep. As a result, when the phrenic nerves are stimulated at TLC, muscle length at equilibrium is approximately 51% of  $L_o$ , and  $P_{di}$  is only 0.04 of the maximal value. The diagram also shows that the amount of muscle shortening during maximal activation at TLC ( $\sim 16\%$   $L_o$ ) is much smaller than that at FRC ( $\sim 40\%$   $L_o$ ), and thus the magnitude of the descent of the dome and the magnitude of  $\Delta P_{ao}$  are also smaller.

As previously pointed out, however, isolated maximal diaphragm activation causes extreme shortening of the muscle fibers and marked distortion of the chest wall. During spontaneous inspiratory efforts, in fact, the diaphragm is never maximally activated (86) and always contracts in a coordinated manner with the intercostal muscles (30, 38, 47). As a result, the degree of diaphragm shortening is smaller, and

measurements in dogs have shown that during such spontaneous efforts, the radius of muscle curvature remains constant (6, 12). Studies of diaphragm silhouette in normal humans using chest radiographs (127, 138), magnetic resonance imaging (82), and computed tomography (139) have also shown that maximal inspiration from FRC to TLC causes little or no change in diaphragm curvature in the coronal plane. Therefore, even though maximal inspiration to TLC produces a decrease in curvature of the human diaphragm in the sagittal plane (82), it appears that  $P_{di}$  during spontaneous inspiratory efforts is primarily or exclusively determined by active muscle length (82, 150).

### Effect of ascites

Accumulation of liquid in the peritoneal cavity commonly occurs as a complicating feature of many diseases of the liver and peritoneum, and studies in dogs have shown that this setting, when produced acutely, has a marked influence on diaphragm mechanics (89, 104, 106). Thus, as the amount of liquid in the cavity gradually increases,  $P_{ab}$  at end-expiration rises, the diaphragm moves cranially, and the ventrolateral wall of the abdomen expands outward. The relaxed diaphragm and abdominal muscles, therefore, lengthen and develop greater passive tension (104, 107), so that the elastance of the abdominal compartment progressively increases (106). In contrast to lung inflation, therefore, the load imposed by the chest wall on the diaphragm is greater, and the load line for the muscle is both displaced upward and more steep, as shown in the diagram (analogous to Fig. 5) given in Figure 6. As a result, the muscle during phrenic nerve stimulation is longer and develops greater force. Specifically, after a moderate amount (100 ml per kg of body weight) of liquid was introduced into the abdominal cavity in supine dogs, the relaxed diaphragm was lengthened to approximately 107% of  $L_o$ , and the muscle during maximal, isolated activation shortened to only approximately 70% of  $L_o$  (104). Consequently, whereas  $P_{di}$  in the control condition was 0.40 of the maximal value, in moderate ascites, it was 0.53 of the maximal value (closed triangle in Fig. 6). It is worth pointing out, however, that, because the amount of diaphragm shortening in ascites is reduced, the descent of the dome is smaller and  $\Delta P_{pi}$  is also smaller. Thus the increase in muscle force translates into a greater  $\Delta P_{ab}$ , but the lung-expanding action of the diaphragm is impaired.

As ascites becomes more severe, the load line for the diaphragm is further displaced upward and steepened, and indeed when the amount of liquid in the dogs was increased to 200 ml per kg of body weight, muscle length during phrenic nerve stimulation was increased to approximately 80% of  $L_o$ . It would be expected, therefore, that the force generated by the muscle would be increased to 0.72 of the maximal value (open square in Fig. 6). However, severe ascites also causes a marked expansion of the lower rib cage and induces an increase in the radius of diaphragm curvature (104). As a result, as occurs during lung inflation,  $P_{di}$  during phrenic nerve stimulation

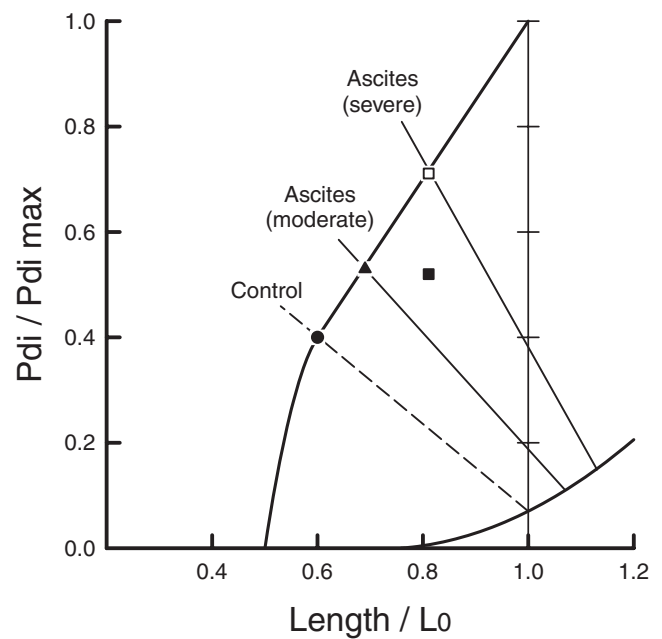


**Figure 6** Graphical analysis of the pressure generated by the diaphragm in the presence of ascites. The continuous lines describing the  $P_{di}$ -length relationships for the maximally active and the passive diaphragm, and the dashed line describing the load line for the isolated diaphragm in the control condition are the same as those in Figure 5. The thin solid lines are the two load lines for the diaphragm in the presence of moderate and severe ascites. With moderate ascites, the relaxed diaphragm lengthens and the elastance of the abdomen increases, so that the load line is displaced upward and is more steep. As a result, the diaphragm during phrenic nerve stimulation shortens less and generates a larger pressure (closed triangle). With severe ascites, the load line is further displaced upward and still more steep, but the radius of diaphragm curvature during phrenic stimulation increases. Consequently, the active diaphragm is even longer, but the pressure generated (closed square) is smaller than anticipated on the basis of muscle length alone (open square).

is smaller than anticipated on the basis of muscle length. In fact,  $P_{di}$  in severe ascites was only 0.51 of the maximal value (closed square in Fig. 6), and the lung-expanding action of the diaphragm was severely impaired (104, 106).

### Interaction between the left and right hemidiaphragms

Although each phrenic nerve in humans supplies its own hemidiaphragm, the  $\Delta P_{di}$  obtained during simultaneous stimulation of the left and right phrenic nerves with single twitches in healthy individuals is greater than the sum of the  $\Delta P_{di}$ 's obtained during their separate stimulation (4). Similarly, when the two phrenic nerves in dogs are stimulated simultaneously at FRC with a frequency of 10 Hz,  $\Delta P_{ao}$  is 10% greater than the sum of the  $\Delta P_{ao}$  values produced by their separate stimulation (37). Moreover, as the frequency of stimulation increases, the  $\Delta P_{ao}$  during simultaneous left and right stimulation increases progressively relative to the sum of the  $\Delta P_{ao}$  produced by their separate stimulation, so that it is approximately 40%



greater than the sum for a stimulation frequency of 30 to 50 Hz (37, 132). Thus the left and right hemidiaphragms have a synergistic interaction, and this implies that the pressure loss induced by a hemidiaphragmatic paralysis is greater than half of the pressure generated by the entire diaphragm. The frequency dependence of the synergism further implies that this additional pressure loss should be particularly prominent when respiratory neural drive is increased, such as during exercise.

Radiographic measurements of the changes in length of the canine diaphragm showed that the active muscle fibers shorten markedly during both unilateral and bilateral phrenic nerve stimulation, but that they tend to shorten less during bilateral stimulation (37). Consequently, the diaphragm would develop greater force during bilateral than during unilateral contraction. Furthermore, and more importantly, the configuration of the diaphragm during unilateral stimulation is very different from that during bilateral stimulation, as shown in Figure 7. That is, during unilateral stimulation, the active hemidiaphragm shortens and moves caudally, while the contralateral, inactive hemidiaphragm is stretched and pulled in both the medial and the caudal direction. The contralateral hemidiaphragm, therefore, develops greater passive tension, and this tension, being transmitted through the central tendon,

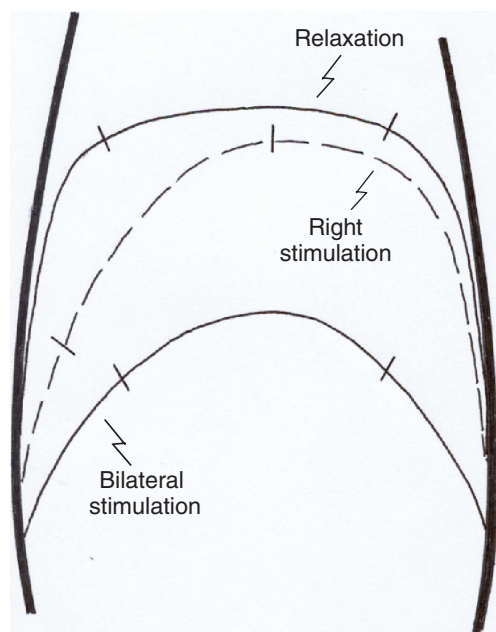


**Figure 7** Contours of the diaphragm seen on anteroposterior radiographs in a dog during relaxation at FRC, during isolated tetanic stimulation of the right phrenic nerve (dashed line), and during combined stimulation of the left and right phrenic nerves. Stimulation frequency = 50 Hz. The two short bars on each contour correspond to the junctions of the muscle fibers with the central tendon and show the lateral shift of the tendon (and the mediastinum) during unilateral phrenic nerve stimulation. The surface area (volume) swept by the diaphragm during simultaneous contraction of the right and left hemidiaphragms is more than twice that swept when the right hemidiaphragm contracts in isolation.

impedes the shortening of the contracting muscle fibers. As a result, the caudal displacement of the contracting hemidiaphragm is reduced, and the volume swept by the diaphragm is less than half that swept when the two hemidiaphragms contract simultaneously (37).

### Role of the mediastinum in the mechanics of the diaphragm

Because isolated activation of a hemidiaphragm in the dog induces a caudal displacement of the contralateral, inactive hemidiaphragm and a lateral shift of the mediastinum toward the active side (Fig. 7) (37), it would be expected that stimulation of one phrenic nerve would produce a fall in  $P_{pl}$  both over the lung apposed to the active hemidiaphragm and over the lung apposed to the inactive hemidiaphragm. To compare the pressure changes occurring over the individual lungs in this condition, two endotracheal tubes were inserted in the right and left main stem bronchi and occluded at end-expiration, and the mean  $\Delta P_{pl}$ 's over the two lungs were assessed by measuring the  $\Delta P_{ao}$ 's in the two tubes (34). When the right or the left phrenic nerve was stimulated,  $\Delta P_{ao}$  on the inactive side was 0.65 times the  $\Delta P_{ao}$  on the active side. However, when the diaphragm was inactive and inspiration was accomplished by the inspiratory intercostal muscles in one hemithorax,  $\Delta P_{ao}$  on the inactive side was, on average, 0.92 times the  $\Delta P_{ao}$  on the active side. On the basis of these observations, it was therefore concluded that the descent of the diaphragm during isolated contraction causes stretching and stiffening of the mediastinum so that the pressure transmission from the ipsilateral to the contralateral pleural cavity is reduced (34). This would imply that the mediastinum exerts a cranially oriented force on the diaphragm; if significant, this force might even prevent the diaphragm from descending excessively during contraction.

Two experiments were performed in an attempt to evaluate the role played by the mediastinum in the mechanics of the canine diaphragm (36). In the first experiment, the mediastinum, including the pericardium, was extensively severed, and  $\Delta P_{ao}$  was measured while the phrenic nerves in the neck were stimulated at different lung volumes between FRC and TLC; diaphragm muscle length in this study was also measured by computed tomography. The  $\Delta P_{ao}$  values and the changes in diaphragm length obtained in these animals were no different from those obtained in animals with an intact mediastinum. The decrease in  $\Delta P_{ao}$  with increasing lung volume was also unaltered. In the second experiment, loads were applied in the caudal direction to the central tendon to establish the force-displacement relationship of the mediastinum, including the attachments of the large vessels and the esophagus to the diaphragm. The results indicated that the canine mediastinum operates on the most compliant part of its force-displacement relationship and that the force it exerts on the diaphragm is small compared with the force developed by the muscle during contraction, except at high lung volumes. Thus

these two experiments collectively lead to the conclusion that, although the mediastinum in the dog is able to sustain significant transmural pressure, it has only a limited influence on the mechanics of the diaphragm.

The extent to which this conclusion also applies to humans is uncertain. It is noteworthy, however, that the ventral part of the mediastinum in humans is considerably thicker than that in the dog. In addition, the central tendon in humans is more firmly attached to the mediastinal structures, in particular the pericardium, than in the dog. It would be reasonable to speculate, therefore, that the mediastinum in humans is stiffer than that in the dog and, thus, that it might impact on the mechanics of diaphragm.

## The Intercostal Muscles

### Functional anatomy

The intercostal muscles form two thin layers that span each of the intercostal spaces. The outer layer, the external intercostals, extends from the tubercles of the ribs dorsally to the costochondral junctions ventrally. The fibers of this layer are oriented obliquely, in the caudal-ventral direction, from the rib above to the rib below. In contrast, the inner layer, the internal intercostals, extends from the chondrosternal junctions to near the tubercles of the ribs, and its fibers run in the caudal-dorsal direction from the rib above to the rib below. Thus, the intercostal spaces contain two layers of intercostal muscle in their lateral portion but a single layer in their ventral portion and sometimes in their dorsal portion as well. Dorsally, in the immediate vicinity of the vertebrae, there may be a small space without internal intercostal muscle fibers. The external intercostal muscle in this area, however, is duplicated in each interspace by the levator costae, a thin, triangular-shaped muscle that originates from the tip of the transverse process of the vertebra and fans out laterally to insert onto the caudal rib. Ventrally, between the sternum and the chondrocostal junctions, the external intercostals are replaced by a fibrous aponeurosis, the anterior intercostal membrane, and the only muscle fibers are those of the internal intercostals. The internal intercostals in this region are distinguished from the interosseous intercostals by both their location and their function (see below) and are conventionally called the “parasternal intercostals.”

Although the external intercostal muscle does not extend to the ventral region of the rib cage, the parasternal intercostals are covered on their inner surface by a thin muscle called the triangularis sterni or transversus thoracis. This muscle is not usually considered among the intercostal muscles, yet its fibers run cranially and laterally from the dorsal aspect of the caudal half of the sternum to the inner surface of the costal cartilages of the third to seventh ribs. These fibers, therefore, are oriented nearly perpendicular to those of the parasternal intercostals and parallel to the external intercostals. All intercostal

muscles, including the triangularis sterni, are innervated by the intercostal nerves.

### Actions of intercostal muscles

#### *The theory of Hamberger*

The actions of the intercostal muscles have been the subject of many diverging theories throughout medical history. Because these theories did not have solid experimental evidence, they will not be examined here. However, even though it was not validated, the theory of Hamberger (85) deserves a special mention because it has provided the basis for conventional thinking of intercostal muscle action for a long time.

This theory is based on an analysis of the model of the ribs and intercostal muscles shown in Figure 8. When an intercostal muscle in one interspace contracts, it pulls the upper rib down and the lower rib up. However, the fibers of the external intercostal slope in the caudal-ventral direction from the rib above to the rib below (Fig. 8A). Therefore, their lower insertion is further from the axis of rotation of the ribs (i.e., the costovertebral articulations) than their upper insertion. Consequently, when these fibers contract, exerting equal and opposite forces at the two insertions, the torque acting on the lower rib, which tends to raise it, is greater than that acting on the upper rib, which tends to lower it. The net

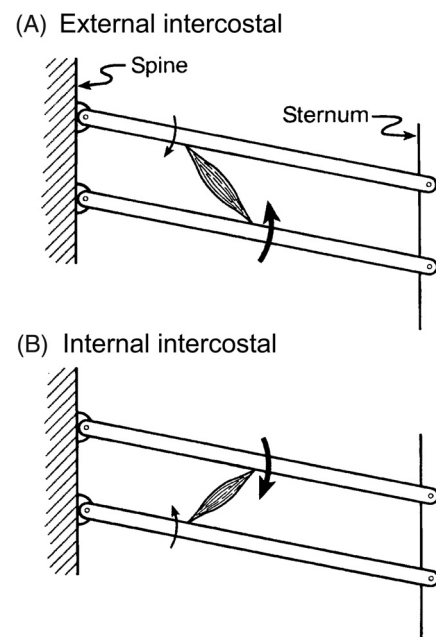


**Figure 8** Diagram illustrating the actions of the intercostal muscles, as proposed by Hamberger (85). The two bars oriented obliquely in each panel represent two adjacent ribs. The external and internal (interosseous) intercostal muscles are depicted as single bundles, and the torques acting on the ribs during contraction of these muscles are represented by arrows. When the external intercostal contracts (A), the torque acting on the lower rib is greater than that acting on the upper rib; the opposite is true when the internal intercostal contracts (B). (Reproduced, with permission, from ref. 47).

effect of the external intercostal, therefore, would be to raise the ribs and to inflate the lung. On the other hand, the fibers of the internal intercostal slope in the caudal-dorsal direction from the rib above to the rib below (Fig. 8B), such that their lower insertion is less distant from the center of rotation of the ribs than their upper insertion. As a result, when this muscle contracts, the torque acting on the lower rib is smaller than that acting on the upper rib, so its net effect would be to lower the ribs and to deflate the lung. Hamberger (85) also concluded that the action of the parasternal intercostals should be referred to the sternum, rather than to the spine. Consequently, even though these muscles are part of the internal intercostal layer, their contraction should raise the ribs and inflate the lung.

The widespread acceptance of the theory of Hamberger as a description of intercostal muscle mechanics has probably been the result of two factors. First, the rib cage is a complex, three-dimensional structure, and the theory provided a simple, convenient, two-dimensional model for this structure. Second, most electrical recordings from intercostal muscles and nerves in animals and from intercostal muscles in humans appeared to be consistent with the conclusions of the theory.

### Respiratory effects of intercostal muscles

Because many intercostal muscles are inaccessible and cannot be activated in isolation, their respiratory action has been assessed by using a standard theorem of mechanics, the reciprocity theorem of Maxwell. When applied to the respiratory system (159, 160), this theorem predicts that the *respiratory effect* of a particular muscle (that is, the  $\Delta P_{ao}$  produced by the muscle during isolated contraction against a closed airway) is related to the mass of the muscle ( $m$ ), the active muscle tension per unit cross-sectional area ( $\sigma$ ), and the fractional change in muscle length ( $\Delta L/L$ ) per unit increase in volume of the relaxed chest wall ( $\Delta V_L$ )<sub>Rel</sub>, such that

$$\Delta P_{ao} = m \sigma [\Delta L / (L \Delta V_L)]_{\text{Rel}} \quad (1)$$

For a machine, such as a lever, mechanical advantage is defined as the ratio of the force delivered at the load to the force applied at the handle. By analogy, the mechanical advantage of a respiratory muscle may therefore be defined as  $\Delta P_{ao} / m \sigma$  and, according to Eq. (1), could be evaluated by measuring  $[\Delta L / (L \Delta V_L)]_{\text{Rel}}$ . In other words, a muscle that shortens during passive inflation (negative  $\Delta L/L$ ) would have an inspiratory mechanical advantage and would cause a fall in  $P_{ao}$  when it contracts alone (inspiratory effect). Conversely, a muscle that lengthens during passive inflation (positive  $\Delta L/L$ ) would have an expiratory mechanical advantage and would cause a rise in  $P_{ao}$  during isolated contraction (expiratory effect).

The validity of Eq. (1) has been tested experimentally on a number of canine respiratory muscles, including the parasternal intercostals and the triangularis sterni, and these observations confirmed the equation in all respects (53, 55, 114). Thus for all these muscles, there was a unique relationship between  $\Delta P_{ao} / m$  during isolated, maximal stimulation

and  $[\Delta L / (L \Delta V_L)]_{\text{Rel}}$ . In addition, the coefficient of proportionality ( $\sigma$ ) between the two variables was  $3.0 \text{ kg/cm}^2$ , in close agreement with values of maximal active muscle tension measured *in vitro* (21, 73, 75, 76). Therefore, to assess the maximal respiratory effects of the external and internal interosseous intercostals in dogs, De Troyer et al. (56) measured the masses of the muscles throughout the rib cage and their fractional changes in length during passive inflation, and for each muscle area, they multiplied  $\Delta L/L$  by  $m$  and by 3.0.

The maximal respiratory effects of the canine external and internal intercostal muscles in the dorsal third, middle third, and ventral third of the even-numbered interspaces are shown in Figure 9. The external intercostal muscle in the dorsal third of the second interspace has a large inspiratory effect (Fig. 9A). However, this inspiratory effect decreases gradually toward the base of the rib cage, such that it is abolished in the 8th interspace and reversed into an expiratory effect in the 10th interspace. Moreover, the external intercostal in any given interspace has a smaller inspiratory effect or a greater expiratory effect as one moves from the angle of the ribs dorsally toward the costochondral junctions. As a result, the external intercostals in the ventral third of the sixth interspace and in the middle and ventral thirds of the 8th and 10th interspaces also have an expiratory effect (56). To the extent that the muscle fibers of the levator costae originate from the transverse process of the vertebra and insert on the caudal rib, the muscle in each interspace must also have an inspiratory effect, but this effect has not been quantified.

On the other hand, the canine internal intercostals in the dorsal third of the rib cage have an expiratory effect (Fig. 9B). However, this expiratory effect decreases gradually from the eighth to the second interspace, and in a given interspace, it decreases progressively from the angle of the ribs to the costochondral junctions. Therefore, the muscle in the middle and ventral thirds of the second interspace has an inspiratory, rather than expiratory, effect (56). For the internal intercostals, in fact, the trend toward a more inspiratory effect continues as one moves further toward the sternum (52). As a result, the parasternal intercostal muscle bundles attached to the costochondral junctions have, on average, no respiratory effect at all, and the muscle bundles in the vicinity of the sternum have a definite inspiratory effect in all interspaces. It is notable, however, that these medial parasternal bundles retain a rostrocaudal gradient (55), such that their inspiratory effect is greatest in the second through fourth interspaces and declines both from the second to the first interspace and from the fourth to the eighth interspace (Fig. 9B). In contrast, the canine triangularis sterni has a large expiratory effect in all interspaces (53).

The respiratory effects of the intercostal muscles in humans were also assessed by applying the reciprocity theorem of Maxwell (54, 163). Thus the muscles were first dissected in cadavers to measure the orientation of the muscle fibers relative to the ribs and to determine muscle masses. The shape of the ribs and their transformation during passive inflation were then determined in healthy individuals by computed

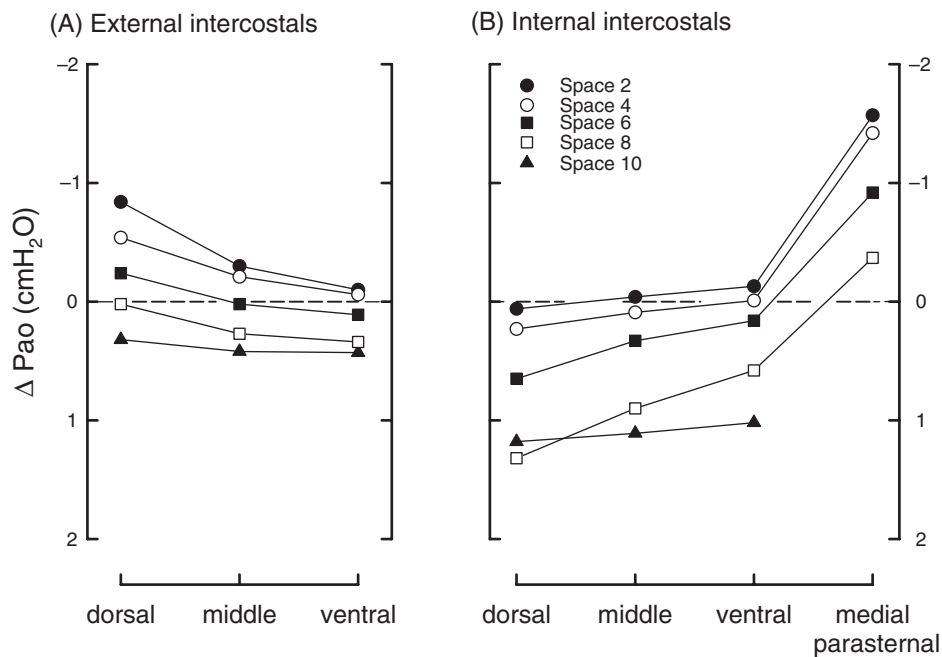


**Figure 9** Maximal respiratory effects of the canine external (A) and internal interosseous (B) intercostal muscles in the dorsal third, middle third, and ventral third of the even-numbered interspaces (both sides of the sternum). The respiratory effects of the medial portion of the parasternal intercostals in interspaces 2, 4, 6, and 8 are also shown. (Reproduced with permission from ref. 47).

tomography, and from these data, the fractional changes in length of lines having the orientation of external and internal intercostal muscles were computed to assess  $[\Delta L/(L\Delta V_L)]_{Rel}$  and to calculate the respiratory effects of the muscles (163). The respiratory effects of the human parasternal intercostals and triangularis sterni were computed similarly by measuring the changes in the angles between the costal cartilages and the sternum during passive inflation (54).

The results of these studies indicated that as in the dog, the parasternal intercostals and the external intercostals in the dorsal portion of the rostral interspaces in humans have inspiratory effects, whereas the internal interosseous intercostals and the triangularis sterni have expiratory effects. Also, as in the dog, the muscles in humans demonstrate prominent rostrocaudal and dorsoventral gradients of respiratory effect. Specifically the inspiratory effect of the human parasternal intercostals decreases from the second to the fifth interspace (54), and that of the external intercostals decreases in both the caudal and the ventral direction, so that it is reversed to an expiratory effect in the ventral portion of the fourth to eighth interspaces (163). These studies, however, also revealed two significant differences relative to the dog. First, the inspiratory effect of the external intercostals in the dorsal portion of a given rostral interspace in humans is much larger than that of the parasternal intercostal in the same interspace, whereas in the dog, it is substantially smaller. This difference is primarily the result of the fact that in contrast to the dog, the mass of external intercostal muscle in humans is much larger than the mass of parasternal intercostal (54, 163). Similarly,

the mass of internal interosseous intercostal muscle in a given caudal interspace in humans is much larger than the mass of triangularis sterni, so their expiratory effect is also much larger. Second, whereas the expiratory effect of the internal interosseous intercostals in the dog is greatest in the dorsal portion of the caudal interspaces, in humans, it is greatest in the ventral portion. This difference might be related to the species difference in rib cage shape and rib displacement.

It is worth emphasizing that the topographic distributions of respiratory effects among the external and internal intercostal muscles, although affected by the distributions of muscle mass, are essentially similar to the topographic distributions of mechanical advantages. Thus, both in humans and in the dog, the areas of external intercostal in the dorsal portion of the rostral interspaces have an inspiratory mechanical advantage, whereas the muscle areas in the ventral portion of the caudal interspaces have an expiratory mechanical advantage. Also, the internal interosseous intercostals in the caudal interspaces have a large expiratory mechanical advantage, but the muscle areas in the ventral portion of the cranial interspaces have a small expiratory or inspiratory mechanical advantage, and the medial portion of the parasternal intercostals in these interspaces have a definite inspiratory mechanical advantage. Inasmuch as the value of mechanical advantage for a particular muscle area is independent of the mass of the muscle and only related to the anatomy of the muscle, as described in Eq. (1), it follows that the distributions of respiratory effects among the intercostal muscles are largely related to the anatomy and kinematics of the rib cage.

## Mechanisms of the respiratory effects

The theory of Hamberger cannot explain the dorsoventral and rostrocaudal gradients of respiratory effect for the external and internal interosseous intercostals. In addition, in several areas of the rib cage, the sign of the respiratory effect of the muscles is opposite to that predicted by the theory. This indicates that the respiratory effects of the intercostal muscles are determined by other factors than the orientation of the muscle fibers alone.

A major shortcoming of the theory of Hamberger is that it is based on a two-dimensional model of the rib cage; the ribs in the model are pictured as rigid straight rods and are assumed to rotate around axes that lie perpendicular to the plane of the ribs (Fig. 8). However, as Saumarez (147) and others (56, 161) have pointed out, real ribs are curved, and this curvature has critical effects on the moments exerted by the intercostal muscles, as shown in Figure 10A. The axis of rib rotation is oriented dorsally and laterally, and at point *a* on the rib, the tangent plane of the rib cage is perpendicular to the axis of rotation. Because the fibers of the external intercostal slope in the caudal-ventral direction from the rib above to the rib below (Fig. 8A), for the portion of the muscle situated at point *a*, the distance between the point of attachment of the muscle on the lower rib and the axis of rib rotation is therefore greater than the distance between the point of attachment of the muscle on the upper rib and the axis of rotation. Consequently, at point *a*, the moment exerted by the external intercostal on the

lower rib is greater than the moment exerted by the muscle on the upper rib, and the net moment is inspiratory. However, at point *b*, the tangent plane of the rib cage lies parallel to the axis of rib rotation, so the distances between the points of attachment of the external intercostal on the two ribs and the axes of rib rotation are equal. Therefore, the net moment exerted by the muscle at point *b* is zero. Thus the net inspiratory moment of the external intercostal is maximum in the dorsal region of the rib cage, decreases to zero at point *b*, and is reversed to an expiratory moment in the ventral region of the rib cage (Fig. 10B). On this basis, the dorsoventral decrease in the inspiratory effect of the external intercostals and the difference between the inspiratory effect of the external intercostals in the dorsal region of the rostral interspaces and the expiratory effect of the triangularis sterni can be understood. Similarly, because the fibers of the internal intercostal slope in the caudal-dorsal direction from the rib above to the rib below (Fig. 8B), the net expiratory moment of the muscle is greatest in the dorsal region, decreases in magnitude as one moves away from the spine, and becomes an inspiratory moment in the vicinity of the sternum (Fig. 10B).

Another shortcoming of the theory of Hamberger is related to the fact that the ribs in the model are linked firmly to each other by the sternum. Such a linkage imposes the constraint that the upper and lower ribs of an interspace have equal compliances. Furthermore, the theory contains the implicit assumption that the coupling between rib displacement and lung volume is the same for the two ribs. Studies of the coupling

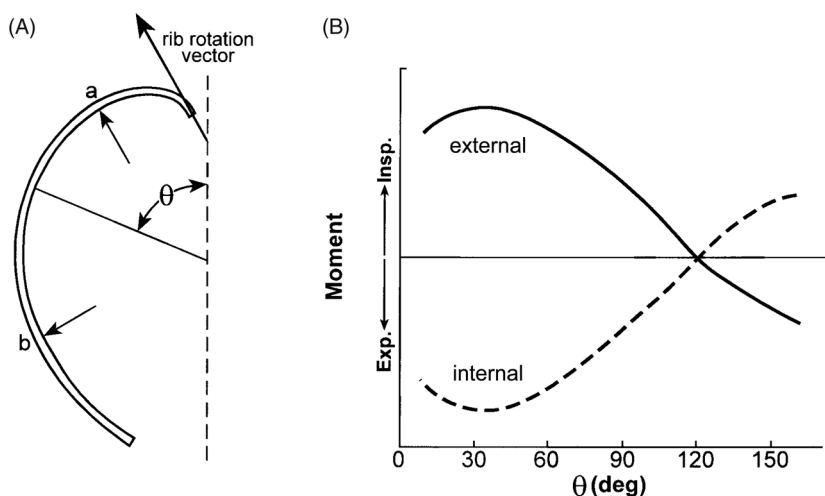


**Figure 10** Effects of rib curvature on the net moment exerted by an intercostal muscle. (A) plan form of a typical rib in the dog and its axis of rotation (bold vector). At point *a*, the distances between the points of attachment of an intercostal muscle on the lower and upper ribs and the axes of rotation are different, and the muscle exerts a net moment on the ribs. At point *b*, however, the distances between the points of attachment of an intercostal muscle on the lower and upper ribs and the axes of rotation of the ribs are equal, and the muscle exerts no net moment. Thus the net moment exerted by the muscle depends on the angular position ( $\theta$ ) around the rib, as shown in (B). The external intercostal muscle (continuous line) has the greatest inspiratory moment in the dorsal portion of the rib cage ( $\theta$  between 15 and 60°); this inspiratory moment then decreases as one moves around the rib cage ( $\theta$  between 60 and 120°) and is reversed into an expiratory moment in the vicinity of the sternum ( $\theta > 120^\circ$ ). The internal intercostal muscle (dashed line in B) shows a similar gradient in expiratory moment. (Reproduced, with permission, from ref. 47).

between the ribs and the lung in dogs have demonstrated, however, that the different ribs have different compliances and are coupled differently to the lung (48, 62, 161).

In these studies, external forces were applied in the cranial direction to individual rib pairs in supine, paralyzed animals with the endotracheal tube occluded at FRC. Cranial rib displacement and  $\Delta P_{ao}$  were measured as the force was increased, and these measurements showed that: (i) for a given force, rib displacement increased progressively with increasing rib number; and (ii) the  $\Delta P_{ao}$  produced by a given rib displacement increased from the second to the fifth rib pair and then decreased markedly from the 5th to the 11th rib pair. As a result, the ratio of  $\Delta P_{ao}$  to applied force also increased with rib number in the more rostral interspaces and decreased markedly in the caudal interspaces, as shown in Figure 11 (closed circles). Therefore, although the forces exerted by a particular intercostal muscle on the upper and lower ribs are equal in magnitude (and opposite in direction), these forces have different effects on the lung. Specifically, in the rostral half of the rib cage, the fall in  $P_{ao}$  produced by the cranial force on a particular rib is larger than the rise in  $P_{ao}$  caused by the caudal force on the rib above. Therefore, a hypothetical intercostal muscle lying parallel to the longitudinal body axis would have a net inspiratory effect during isolated contraction. On the other hand, in the caudal half of the rib cage, the fall in  $P_{ao}$  produced by the cranial force on a particular rib is much smaller than the rise in  $P_{ao}$  produced by the caudal force

on the rib above, so an intercostal muscle lying parallel to the longitudinal body axis would have a net expiratory effect.

This nonuniform coupling between the ribs and the lung is probably related to differences between the areas of the lung subtended by the different ribs (62). In the dog, the radii of the ribs in the rostral half of the rib cage increase gradually with increasing rib number (123). In this half of the rib cage, therefore, the area of the lung subtended by a particular rib should be greater than that subtended by the rib above, so it would be expected that for a given displacement, this particular rib would induce a larger  $\Delta P_{ao}$  than the rib above. On the other hand, the radii of the ribs in the caudal half of the rib cage still increase with increasing rib number, but these ribs are in part apposed to the abdomen, rather than the lung (129, 130). At FRC, the most caudal ribs are even entirely apposed to the abdomen. Consequently, the primary effect of a cranial displacement of these ribs is an expansion of the ventral abdominal wall and a fall in  $P_{ab}$ ; the fall in  $P_{ao}$  that takes place is only secondary, due to the (passive) caudal displacement of the diaphragm (48).

On the basis of these observations, the conclusion can therefore be drawn that the respiratory effects of the intercostal muscles are the result of two mechanisms (47, 161). The predominant mechanism is the nonuniform coupling between rib displacement and lung expansion. This mechanism has a larger effect in the ventral region of the rib cage than in the dorsal region, and both in humans and in the dog, it confers an inspiratory bias to the external and internal interosseous intercostals in the rostral interspaces and an expiratory bias to both muscles in the caudal interspaces. The second mechanism is related to the orientation of the muscle fibers, as inferred by Hamberger. Because of the three-dimensional configuration of the rib cage, however, the magnitude of the effect of this mechanism is larger in the dorsal region of the rib cage than in the ventral region, and its direction is reversed in the vicinity of the costochondral junctions. It thus accounts not only for the difference between the external and internal intercostals in the dorsal portion of the rib cage, but also for the difference between the interosseous and intercartilaginous portions of the internal intercostals and that between the external intercostals and the triangularis sterni. Although these two mechanisms operating together account well for the respiratory effects of the intercostal muscles in most interspaces (161), it must be stressed that they do not explain the large expiratory effect of the muscles in the most caudal interspaces. At this point, the mechanism for these large expiratory effects is still unclear. The mechanism for the larger expiratory effect of the internal interosseous intercostals in the ventral, rather than dorsal portion of the caudal interspaces in humans is also uncertain.

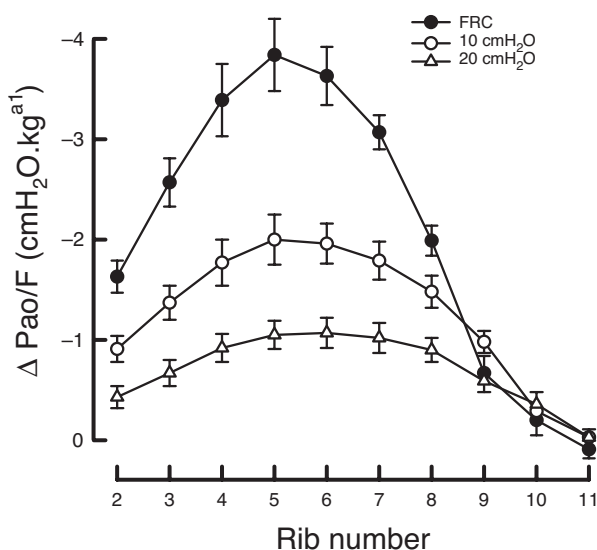


**Figure 11** Effect on the lung of external loading of individual rib pairs in the cranial direction. Data are the mean  $\pm$  SE values of the changes in airway opening pressure ( $\Delta P_{ao}$ ) per unit force (F) on the ribs obtained from seven animals. At FRC (closed circles),  $\Delta P_{ao}/F$  increases from the second to the fifth rib pair and then decreases continuously to the eleventh rib pair.  $\Delta P_{ao}/F$  for ribs 2 to 8, however, decreases markedly when lung volume is passively increased from FRC to 10 cmH<sub>2</sub>O (open circles) and 20 cmH<sub>2</sub>O (open triangles) transrespiratory pressure. (Reproduced, with permission, from ref. 48).

### Implications of the respiratory effects

The finding that in the dog, both the external intercostals and the internal interosseous intercostals have an inspiratory effect in some areas and an expiratory effect in other areas

implies that the function of these muscles during breathing depends on the topographic distribution of neural drive. For example, if the external intercostals in the dorsal region of the rostral interspaces were active during the inspiratory phase of the breathing cycle, they would cause lung inflation. However, if the external intercostals in the ventral region of the caudal interspaces were active during the expiratory phase of the cycle, they would produce lung deflation. Similarly, activation of the internal interosseous intercostals in the caudal interspaces during expiration would deflate the lung, but activation of the internal intercostals in the ventral region of the most rostral interspaces during inspiration would inflate the lung. The respiratory effects of the external intercostals in humans similarly imply that the muscles could have an inspiratory function, an expiratory function, or both, depending on the spatial distribution of neural drive during inspiration and expiration.

### Distribution of neural drive to the intercostal muscles

A number of electromyographic studies in dogs (45), cats (84), and humans (30, 38, 80, 156) have shown that the parasternal intercostals invariably contract during the inspiratory phase of the breathing cycle. In the dog, inspiratory activity in a particular parasternal intercostal, in fact, is greatest in the muscle bundles situated in the vicinity of the sternum, and it decreases progressively in the lateral direction such that the muscle bundles near the chondrocostal junctions remain consistently silent (52). Also, inspiratory activity in the medial parasternal bundles in the dog is greatest in the second through the fifth interspace and decreases gradually from the fifth to the eighth interspace and from the second to the first interspace as well (110, 112). Thus the spatial distribution of neural drive among the canine parasternal intercostals mirrors the spatial distribution of inspiratory mechanical advantage and inspiratory effect. The spatial distribution of neural inspiratory drive to the parasternal intercostals in humans also matches the spatial distribution of the inspiratory mechanical advantage and inspiratory effect of the muscles, with a gradual decrease from the first to the fifth interspace (79). Such a distribution of neural inspiratory drive must confer to the muscles a definite inspiratory function during breathing.

Similarly, electrical recordings from intercostal muscles and nerves in anesthetized cats and dogs, combined with selective denervation procedures, have shown that the external intercostal and levator costae muscles are active only during inspiration (3, 42, 84, 88, 98, 111, 148). These recordings have also demonstrated that external intercostal inspiratory activity in these animals is greatest in the dorsal region of the most rostral interspaces and declines gradually in the caudal direction. External intercostal inspiratory activity in a particular rostral interspace also decreases from the dorsal to the lateral region and decreases further from the lateral to the ventral region (111). Thus, as is the case for the parasternal intercostals, the spatial distribution of inspiratory activity among the exter-

nal intercostals in quadrupeds mirrors the spatial distribution of the magnitude of the muscle inspiratory mechanical advantage and inspiratory effect. The external intercostals with an expiratory effect, that is, in the ventral region of the caudal interspaces, are never active during breathing, including when the demand placed on the respiratory muscle pump is increased by CO<sub>2</sub>-enriched gas mixtures or by external mechanical loads (111). The topographic distribution of neural inspiratory drive to the external intercostals in humans is similar to that in the dog (44), and this implies that both in quadrupeds and in humans, these muscles also have an inspiratory function during breathing.

On the other hand, the triangularis sterni (58, 91) and the internal interosseous intercostals (3, 84, 111) in the cat and in the dog are active only during expiration, and the spatial distribution of internal intercostal expiratory activity mirrors the spatial distribution of the muscle expiratory mechanical advantage. Thus internal intercostal expiratory activity is greatest in the dorsal portion of the caudal interspaces, and it decreases gradually in the rostral and the ventral direction. The areas of internal interosseous intercostal muscle with an inspiratory mechanical advantage, that is, in the middle and ventral portions of the most rostral interspaces, remain silent during breathing (111). In quadrupeds, therefore, the triangularis sterni and the internal interosseous intercostals have a definite expiratory function during breathing.

In summary, the parasternal intercostals and levator costae have an inspiratory function during breathing, whereas the triangularis sterni has an expiratory function. Although the spatial distribution of expiratory activity among the internal interosseous intercostals in humans is not known, the external intercostals and internal interosseous intercostals also have, respectively, inspiratory and expiratory functions during breathing. These conclusions fully agree with those of the theory of Hamberger. However, whereas the theory maintains that the opposite functions of the external and internal interosseous intercostals are the result of the orientation of the muscle fibers alone, they are primarily the result of selective regional activation of the muscles. As discussed in a recent review article (47), the topographic distribution of neural drive among the intercostal muscles appears to be largely determined by central, as opposed to peripheral, control mechanisms.

### Mechanical interactions among the inspiratory intercostal muscles

#### *Interactive effects on the rib cage*

The lung-expanding action of the parasternal intercostals and the external intercostals in the dorsal portion of the rostral interspaces is the result of the rib elevating action of the muscles. Indeed, the ribs provide the solid structural elements that allow for the transformation of intercostal muscle tension into lung expansion, and when the bony ribs are removed in dogs, so that the lateral walls of the rib cage simply consist

of bands of periosteum connected by intercostal muscles, the fall in  $P_{ao}$  produced by contraction of the rostral external intercostals is reversed into a pressure rise (18). It has to be noted, however, that, although the fall in  $P_{pl}$  produced by the parasternal and external intercostals in intact animals is the result of the elevation of the ribs, this pressure fall, in turn, opposes the rib elevation (50). The effect of  $\Delta P_{pl}$  on the ribs during contraction of the inspiratory intercostals is essentially identical to its effect during contraction of the diaphragm (see section *Mechanisms of action of the diaphragm on the rib cage*).

Notwithstanding the role of  $\Delta P_{pl}$  in determining rib displacement, when either the parasternal intercostals or the external intercostals in the dog contract in isolation in all interspaces, all the ribs are displaced cranially and outward (42, 61, 121). As shown in Figure 12, however, the two sets of muscles drive the ribs along different trajectories. Specifically, when the parasternal intercostals in all interspaces are

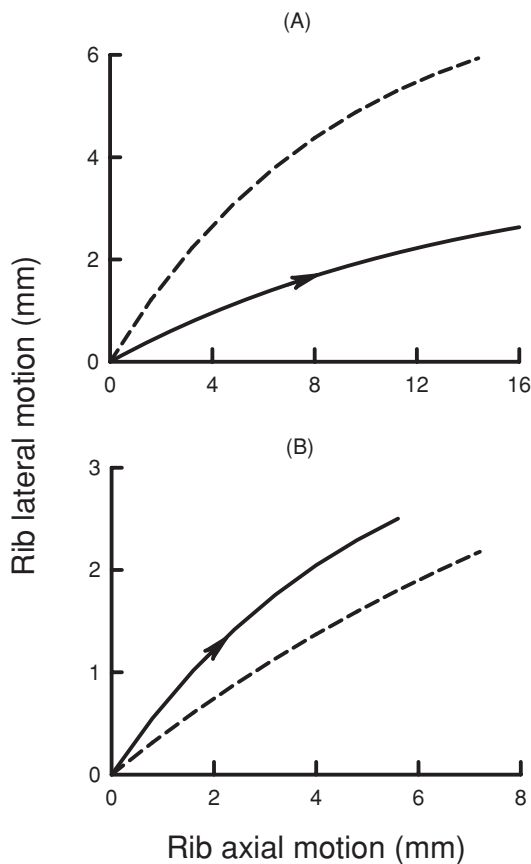


**Figure 12** Patterns of rib displacement produced by the external and parasternal intercostals in the dog. In the animal in (A), the parasternal intercostals in interspaces 1 to 8 were denervated on both sides of the sternum; in the animal in (B), the parasternal intercostals were intact but the external intercostals in interspaces 1 to 8 were excised. Both animals had complete diaphragmatic paralysis. The dashed line in each panel is the trajectory of the ribs during passive inflation (relaxation), and the solid line with the arrowhead corresponds to a spontaneous inspiration. (Reproduced, with permission, from ref. 61).

bilaterally denervated in dogs with diaphragmatic paralysis, such that the external intercostals and levator costae are the only muscles active during inspiration, the cranial displacement of the ribs is substantially greater than their outward displacement relative to the rib trajectory during passive inflation (Fig. 12A). In contrast, when the parasternal intercostals in dogs with diaphragmatic paralysis are maintained intact and the external intercostals and levator costae in all interspaces are excised, such that the parasternal intercostals are the only muscles active during inspiration, the outward displacement of the ribs is greater than their cranial displacement relative to the relaxation trajectory (Fig. 12B). Yet, when the external intercostals, levator costae, and parasternal intercostals contract together in a coordinated manner, the trajectory of the ribs lies very near their relaxation trajectory (61).

Using a finite element analysis, Loring (118) inferred that as in the dog, the parasternal intercostals in humans displace the ribs cranially and outward whereas the external intercostals displace the ribs only cranially. Also, measurements of the changes in rib cage dorsoventral and lateral diameters in seated normal subjects have shown that the displacement of the rib cage during resting breathing is similar to that during passive inflation (39, 99, 125). Thus both in the dog and in humans, the coordinated activation of the two sets of inspiratory intercostals during breathing drives the ribs along a trajectory that matches the relaxation trajectory and thereby reduces the work of breathing (2, 128).

The parasternal intercostals and external intercostals displace the sternum differently as well. Because the parasternal intercostals run obliquely in the caudal-lateral direction from the sternum to the costal cartilages, their isolated contraction in one or two interspaces in the dog causes a cranial and outward displacement of the ribs together with a caudal displacement of the sternum (45). In contrast, the external intercostals and levator costae act on the sternum through their action on the ribs, so their isolated contraction displaces the sternum in the cranial direction (42, 61). The sternum in the dog and in the cat also moves in the cranial direction during passive inflation, but it moves in the caudal direction during spontaneous, coordinated contraction of the parasternal and external intercostals (28, 45). Thus, in these animals, coordinated intercostal muscle activation during breathing drives the ribs but not the sternum along the relaxation trajectory, and this distortion of rib cage kinematics implies an increase in the work of breathing. In humans, however, such a distortion does not occur and the sternum moves in the cranial direction during both spontaneous inspiration and passive inflation (39), as discussed below.

### *Interactive effects on the lung*

As for the other skeletal muscles, including the diaphragm (75, 126), the force developed by a particular parasternal or external intercostal muscle bundle during isometric contraction *in vitro* varies as a function of the length of the muscle (74). To the extent that the different intercostal muscles



are interconnected by the ribs, the costal cartilages, and the sternum, it would therefore be expected that the length of a particular muscle and, hence, the force exerted by this muscle during contraction would depend on the interactions between the muscle and the other intercostal muscles contracting at the same time as well as on the forces developed by these other muscles.

To assess the interactions between the different inspiratory intercostals on the lung, Legrand et al. (116) induced electrical stimulation of the parasternal intercostals and the interosseous (both external and internal) intercostals in dogs with the endotracheal tube occluded, first in two interspaces separately and then in the same two interspaces simultaneously. The  $\Delta P_{ao}$  obtained during simultaneous stimulation of the muscles in two interspaces was, within 10%, equal to the sum of the  $\Delta P_{ao}$  values obtained during their separate stimulation. The  $\Delta P_{ao}$ 's produced by the simultaneous contraction of the parasternal or interosseous intercostals in one or two interspaces on the left and right sides of the sternum were also nearly equal to the sum of the  $\Delta P_{ao}$ 's produced by separate left and right contraction (17). Thus, whereas the two hemidiaphragms have a synergistic interaction on the lung (37, 132), the pressure changes generated by the different inspiratory intercostals are essentially additive, and the potential synergistic or antagonistic interactions between them are negligible.

Based on these observations, one may therefore estimate, both in the dog and in humans, the total  $\Delta P_{ao}$  that would be generated by a maximal, simultaneous contraction of the parasternal intercostals in all interspaces and the total  $\Delta P_{ao}$  that would be generated by a maximal contraction of all the areas of external intercostal muscle with an inspiratory effect. If the  $\Delta P_{ao}$  generated by the areas of external intercostal muscle in the dorsal third, the middle third, and the ventral third of the second interspace in the dog (data shown in Fig. 9A) are added to each other, it appears that the total inspiratory effect of the muscle ( $-1.2 \text{ cmH}_2\text{O}$ ) is close to that of the sternal portion of the parasternal intercostal in the same interspace ( $-1.6 \text{ cmH}_2\text{O}$ ). However, as is shown in Figure 13A, the inspiratory effect of the external intercostals decreases rapidly from the second to the sixth interspace. The inspiratory effect of the sternal half of the canine parasternal intercostals also decreases from the second to the eighth interspace, but it decreases less than that of the external intercostals. As a result, if the  $\Delta P_{ao}$  values calculated for the different even-numbered interspaces are added to each other and multiplied by two for the odd-numbered interspaces, the total  $\Delta P_{ao}$  value obtained for all the canine external intercostals with an inspiratory effect is  $-4.6 \text{ cmH}_2\text{O}$ , whereas the total  $\Delta P_{ao}$  value obtained for the parasternal intercostals in all interspaces amounts to  $-8.6 \text{ cmH}_2\text{O}$ .

In contrast, the external intercostals in humans are thicker and have a much greater mass than the parasternal intercostals, so that the external intercostal in each interspace down to the sixth has a much greater inspiratory effect than the parasternal intercostal (Fig. 13B). In addition, whereas the external intercostals in the dorsal region of the rib cage retain an inspiratory

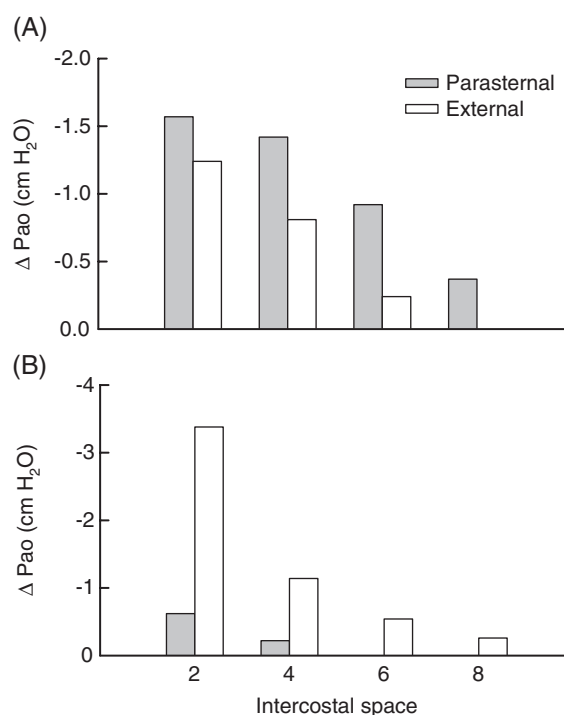


**Figure 13** Maximal inspiratory effects of the parasternal intercostal and external intercostal muscles in the even-numbered interspaces in dogs (A) and in humans (B). (Redrawn from ref 47, with permission).

effect down to the eighth interspace (163), the parasternal intercostals in humans do not extend beyond the fifth interspace. In humans, therefore, the total  $\Delta P_{ao}$  value calculated for all the areas of external intercostal muscle with an inspiratory effect would be approximately  $-15 \text{ cmH}_2\text{O}$ , whereas the total  $\Delta P_{ao}$  value calculated for the parasternal intercostals in all interspaces would be only  $-2$  to  $-3 \text{ cmH}_2\text{O}$ . The greater inspiratory effect of the external intercostals compared to the parasternal intercostals in humans, combined with the large neural inspiratory drive to the external intercostals in the dorsal region of the rostral interspaces (44), might account in part for the fact that the sternum in humans moves cranially, rather than caudally, during inspiration (39).

### Effect of lung inflation

DiMarco et al. (64) examined the lung-volume dependence of the action of the parasternal and external intercostals by introducing a stimulating electrode in the upper epidural space in anesthetized dogs. They then applied trains of rectangular pulses to the spinal cord while the animal was apneic and the endotracheal tube was occluded at different lung volumes. As shown in Figure 14 (closed circles), when the epidural stimulation was delivered at FRC,  $\Delta P_{ao}$  was  $-15.5 \pm 0.9 \text{ cmH}_2\text{O}$ ; this value is remarkably close to that calculated on the basis of the individual respiratory effect of the different muscle areas (see above). However, when lung volume before stimulation was increased above FRC by applying a

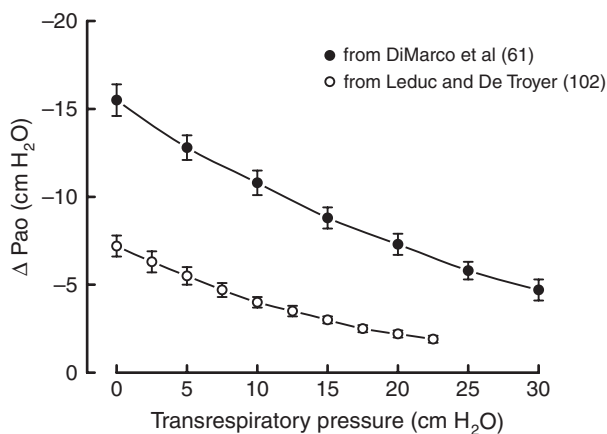


**Figure 14** Effects of inflation on the pressure-generating ability of the inspiratory intercostals. The closed circles are the mean  $\pm$  SE values of  $\Delta P_{ao}$  obtained from 19 dogs during isolated, tetanic stimulation of the inspiratory (and expiratory) intercostals at different lung volumes, as reported by DiMarco et al. (64). The open circles are the mean  $\pm$  SE values of  $\Delta P_{ao}$  obtained from 9 dogs during spontaneous contraction of the parasternal intercostals alone (105). Similar to the diaphragm, the pressure-generating ability of the inspiratory intercostals decreases with increasing lung volume. (Reproduced with permission from ref. 63).

transrespiratory pressure of +10 cmH<sub>2</sub>O,  $\Delta P_{ao}$  was reduced to  $-10.8 \pm 0.7$  cmH<sub>2</sub>O, and when lung volume was increased further to a transrespiratory pressure of +30 cmH<sub>2</sub>O,  $\Delta P_{ao}$  was only  $-4.7 \pm 0.6$  cmH<sub>2</sub>O. DiMarco et al. (64) subsequently repeated the procedure after the internal intercostal nerves in interspaces 1 to 6 were sectioned at the costochondral junction. The parasternal intercostals and the triangularis sterni, therefore, were denervated, and the stimulations affected only the interosseous intercostals. Although the  $\Delta P_{ao}$  values in this condition were smaller than the values before denervation, the influence of lung volume was the same.

This decrease in  $\Delta P_{ao}$  with increasing lung volume might have been the result of an increase in the effect of the expiratory intercostals. Indeed, stimulating the spinal cord through an electrode in the upper epidural space produces a strong, simultaneous activation not only of the parasternal and external intercostals over a large fraction of the rib cage, but also of the internal interosseous intercostals and the triangularis sterni. Moreover, when lung volume in dogs is passively increased above FRC, the internal interosseous intercostals in many interspaces and the triangularis sterni lengthen significantly (53, 56). Therefore, in accordance with the length-tension characteristics of skeletal muscles, the force exerted by these expiratory muscles in response to a given activation should increase, and the fall in  $P_{ao}$  obtained during spinal cord stimulation should decrease.

In a subsequent study, however, Ninane and Gorini (136) produced selective activation of the canine parasternal intercostals by electrical stimulation of the internal intercostal nerves at the costochondral junction. The triangularis sterni in these animals was sectioned and did not, therefore, confound the pressure measurements. Yet, the  $\Delta P_{ao}$  obtained during

stimulation at a transrespiratory pressure of +15 cmH<sub>2</sub>O was approximately 50% of the value obtained during stimulation at FRC. Also, in a more recent study, Leduc and De Troyer (105) excised the external intercostal muscles in all interspaces in dogs with complete diaphragmatic paralysis and bilateral vagotomy, and they measured  $\Delta P_{ao}$  while the animals performed spontaneous inspiratory efforts against an occluded endotracheal tube at different lung volumes. Consequently, the parasternal intercostals in these animals were the only muscles active during inspiration, the muscles contracted in all interspaces in a coordinated manner, and the normal spatial distribution of neural drive among them was maintained. Although inspiratory EMG activity in the parasternal intercostals remained unchanged with increasing lung volume (i.e., neural drive to the muscles was constant),  $\Delta P_{ao}$  decreased markedly and continuously as lung volume before occlusion increased (Fig. 14, open circles). These observations provide unequivocal evidence, in agreement with the conclusion of DiMarco et al. (64), that inflation does adversely affect the pressure-generating capacity of the parasternal intercostals.

By analogy with the lung-volume dependence of  $P_{di}$ , the lung-volume dependence of the pressure-generating ability of the inspiratory intercostals was initially attributed to the decrease in active muscle length (64). To be sure, both the parasternal intercostals and the external intercostals in the rostral interspaces shorten with lung inflation (55, 56, 65). However, whereas the canine diaphragm shortens by approximately 30% of  $L_{FRC}$  during passive inflation from FRC to TLC (51, 75, 134, 152, 158), the inspiratory intercostals shorten by 10% or less. Furthermore, in supine dogs, the resting  $L_{FRC}$  of the external intercostals in the rostral interspaces may be close to  $L_o$ , but the resting  $L_{FRC}$  of the parasternal intercostals is approximately 15% longer than  $L_o$  (74). Therefore, even though the canine parasternal intercostals might be shorter during strong contraction at high lung volumes than during strong contraction at FRC, it would be expected that they would remain relatively close to  $L_o$  at all lung volumes and that their force-generating capacity would be preserved. The finding by Decramer and colleagues (29, 95) that the parasternal intercostals in the dog generate a similar or slightly greater force on the ribs during stimulation near TLC than during stimulation at FRC supports this view. The detrimental effect of inflation on the capacity of these muscles to generate a  $\Delta P_{pl}$  must, therefore, be the result of other mechanisms.

As we pointed out in section *Graphical representation of diaphragm action*, in supine dogs, the relaxed diaphragm at FRC is stretched by the action of gravity on the abdominal content. Consequently, it develops passive tension, and this passive tension decreases gradually as lung volume is passively increased above FRC and the muscle shortens. As a result, the elastance of the relaxed diaphragm decreases. During isolated contraction of the inspiratory intercostals at high lung volumes, therefore, a given  $\Delta P_{ao}$  causes a larger cranial displacement of the passive diaphragm than it does during contraction of the muscles at FRC, leading to a greater loss in  $\Delta P_{ao}$  (48, 105). This mechanism, however, accounts

for less than one-half the total decrease in the pressure-generating capacity of the inspiratory intercostals at high lung volumes.

A major determinant of this decrease was identified in a study of the effect of lung inflation on the coupling between the ribs and the lung (48). The experimental protocol followed in this study was similar to that described in section *Mechanisms of the respiratory effects*, but in this case, the external, cranially oriented forces were applied to the ribs first at FRC, then after passive inflation to a transrespiratory pressure of +10 cmH<sub>2</sub>O, and finally after passive inflation to a transrespiratory pressure of +20 cmH<sub>2</sub>O. Such loading reproduces the pattern of rib displacement caused by the external intercostals (61). As shown in Figure 11, for all the ribs situated cranial to the zone of apposition (ribs 2 to 8), the  $\Delta P_{ao}$  produced by a given force decreased markedly with increasing lung volume. Because the forces applied to the ribs were the same at all lung volumes, this decrease in  $\Delta P_{ao}$  could not be related to the length-tension characteristics of the muscles. On the other hand, because the ribs move primarily through a rotation around the axis of their neck, they become oriented more transversely relative to the sagittal midplane as they rotate cranially with lung inflation. A given cranial rib displacement, therefore, is associated with a smaller outward displacement, as shown in Figure 15. In fact, at 20 cmH<sub>2</sub>O transrespiratory pressure, the outward rib displacement produced by a given force was nearly abolished whereas the cranial rib displacement was only moderately reduced (48). An identical alteration in the pattern of rib displacement was also observed during isolated, spontaneous contraction of the parasternal intercostals at high lung volumes (105). Because in the dog, a given rib displacement in the outward direction is about four times more effective in increasing lung volume

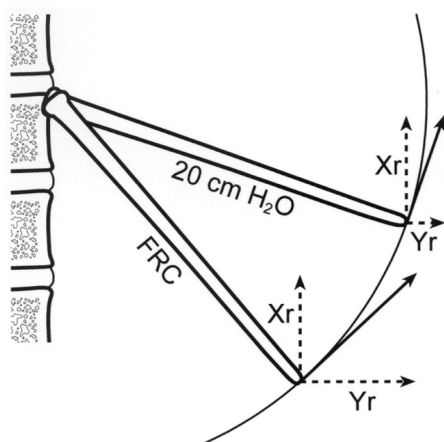


**Figure 15** Dorsal view of the spine and one rib in its position at FRC and its position at 20 cmH<sub>2</sub>O transrespiratory pressure. Because the rib at FRC is slanted caudally, it moves both cranially (X<sub>r</sub>) and outward (Y<sub>r</sub>) during cranial loading. However, at 20 cmH<sub>2</sub>O transrespiratory pressure, the rib is almost horizontal. Therefore, loading the rib causes a cranial displacement with little or no outward displacement. (Reproduced with permission from ref. 48).

than the same rib displacement in the cranial direction (61), this change in the direction of rib displacement must cause a substantial decrease in  $\Delta P_{ao}$ . Thus, in the dog, the pressure-generating ability of the inspiratory intercostals acting alone decreases with increasing lung volume partly because the elastance of the diaphragm decreases, but mostly because the direction of rib displacement is altered.

The effect of lung volume on the pressure-generating capacity of the intercostal muscles in humans is uncertain. Also, the orientation of the ribs and the axes of rib rotation in humans are different from those in the dog, and it is difficult to predict the relative effectiveness of the outward vs. cranial displacement of the human ribs in increasing lung volume. However, the rotation of the human ribs during passive inflation (163) is similar in magnitude to that observed in the dog (123). Therefore, it would be expected that an increase in lung volume in humans would also reduce the outward displacement of the ribs and, with it, the lung-expanding action of the muscles.

## Interaction between the Diaphragm and the Inspiratory Intercostals

### Interactive effects on the chest wall

Coordinated contraction of the parasternal and external intercostals thus produces expansion of the lung by elevating the ribs and expanding the rib cage. When these muscles contract alone, however, the fall in  $P_{pl}$  is transmitted through the relaxed diaphragm to the abdominal cavity. As a result,  $P_{ab}$  also falls, and the abdominal wall moves inward. This pattern is typically observed in animals (29, 45) and in humans (87, 100, 135) with diaphragmatic paralysis. Conversely, when the diaphragm contracts alone, such as in subjects with quadriplegia, it produces a rise in  $P_{ab}$  and a large expansion of the abdominal wall, but the fall in  $P_{pl}$  induces an inward displacement of the rostral half of the rib cage (22, 69, 133, 154). Passive inflation, however, causes simultaneous expansion of the rib cage and abdominal wall, and coordinated contraction of the diaphragm and inspiratory intercostals during resting breathing in supine anesthetized dogs with all respiratory muscles intact (29, 45) and in seated healthy humans (39, 99, 125, 141) has the same effect. In these conditions, the chest wall displacement observed during a quiet inspiration is, in fact, nearly superimposed on the relaxation trajectory. Thus isolated contraction of either the inspiratory intercostals or the diaphragm causes substantial chest wall distortion, and coordinated contraction of the two sets of muscles reduces the elastic work of breathing for a given lung expansion.

### Interactive effects on the lung

To examine the interaction between the inspiratory intercostals and the diaphragm on the lung, DiMarco et al. (66) induced, first separately and then simultaneously, electrical

stimulation of the diaphragm in anesthetized dogs by applying trains of rectangular pulses to the phrenic nerves in the neck and electrical stimulation of the intercostal muscles by applying trains of similar pulses to the spinal cord through an electrode positioned in the epidural space. All stimulations in this study were also performed while the animal was apneic and the endotracheal tube was occluded. When the diaphragm and intercostal muscles were made to contract simultaneously at FRC,  $\Delta P_{ao}$  was 17% greater than the sum of the  $\Delta P_{ao}$  values produced by their separate contractions. As lung volume increased above FRC,  $\Delta P_{ao}$  during combined diaphragm-intercostal activation increased progressively relative to the sum of the  $\Delta P_{ao}$  produced by their separate activations, so that it was 90% greater than the sum when transrespiratory pressure before contraction was increased to +30 cmH<sub>2</sub>O. Conversely, when lung volume was decreased below FRC by applying a transrespiratory pressure of -10 cmH<sub>2</sub>O,  $\Delta P_{ao}$  during combined activation was equal to the sum of the  $\Delta P_{ao}$  obtained during separate activation. DiMarco et al. (66) concluded, therefore, that the interaction between the diaphragm and the inspiratory intercostals on the lung is synergistic, and that the degree of synergism increases with increasing lung volume.

DiMarco et al. (66) also measured the changes in length of the diaphragm and parasternal intercostals in these experiments. The two muscles shortened markedly during both combined and isolated activation at all lung volumes, but they both shortened less in the first instance than in the second. On the basis of this observation, the investigators further concluded that the synergism between the diaphragm and the inspiratory intercostals is largely related to the length-tension characteristics of the muscles. That is, because the inspiratory intercostals prevent the diaphragmatic muscle fibers from shortening excessively during contraction, the diaphragm would develop greater pressure during combined activation than it does during isolated activation. Similarly, by impeding shortening of the inspiratory intercostals, the active diaphragm would allow these muscles to develop greater force.

To be sure, the fall in  $P_{pl}$  during combined diaphragm-intercostal activation is greater than during activation of the diaphragm alone. Consequently, the load on the diaphragm is greater, so that the amount of muscle shortening is reduced and the force exerted by the muscle in response to a given activation is greater. Because the amount of muscle shortening is reduced,  $\Delta P_{ab}$  is smaller and, hence, all the increase in muscle force translates into a greater  $\Delta P_{pl}$  (or  $P_{ao}$ ). In addition, by reducing the shortening of the diaphragm, contraction of the inspiratory intercostals should also reduce, if not abolish, the increase in the radius of diaphragm curvature that takes place during isolated, supramaximal phrenic nerve stimulation at high lung volumes (6, 63). During combined diaphragm-intercostal activation, therefore, the diaphragm would generate a larger  $\Delta P_{ao}$  at FRC than it does during isolated contraction, and the adverse effect of increasing lung volume on this  $\Delta P_{ao}$  would be attenuated.

Furthermore, as pointed out in section *Effect of lung inflation*, isolated contraction of the inspiratory intercostals at FRC causes a cranial displacement of the relaxed diaphragm, which leads to a loss in  $\Delta P_{ao}$ . Also, in supine dogs, the elastance of the relaxed diaphragm decreases as lung volume is passively increased above FRC. For a given  $\Delta P_{ao}$ , therefore, the cranial displacement of the relaxed diaphragm produced by an isolated contraction of the inspiratory intercostals is larger at high lung volumes than at FRC, so that the pressure loss is greater (48, 105). Because the diaphragm has a greater elastance during contraction than during relaxation, concomitant activation of the diaphragm should reduce or abolish this pressure loss. As a result, contraction of the inspiratory intercostals at FRC produces a larger  $\Delta P_{ao}$  when it occurs in the presence of a concomitant contraction of the diaphragm than it does in the presence of an inactive diaphragm (49), and it would be expected that this difference in  $\Delta P_{ao}$  would proportionately increase with increasing lung volume. On this basis, it would be reasonable to conclude that both the diaphragm and the intercostals participate in the synergism that occurs during their simultaneous activation and in the lung volume dependence of that synergism.

## The Neck Muscles

### Functional anatomy

There are many muscles that connect the head and the rib cage or the cervical spine and the rib cage, but of all these muscles, only the scalenes and the sternomastoids have a significant respiratory function. The scalenes in humans consist of three muscle heads that run from the transverse processes of the lower five cervical vertebrae to the upper surface of the first two ribs and are innervated from the lower five cervical segments, whereas the sternomastoids are primarily supplied by the 11th cranial nerve and run from the mastoid process to the ventral surface of the manubrium sterni and the medial third of the clavicle. The muscles in the dog have a similar overall anatomical arrangement, but the medial head of the scalenes in this animal (the so-called "pars supracostalis") descends to the lateral aspect of the sixth to eighth ribs, rather than the first rib (46); in the hamster, this medial head descends only to the third and fourth ribs (78).

### Respiratory action of the neck muscles

When the head and the cervical spine in the dog are fixed, isolated contraction of either the scalenes or the sternomastoids by electrical stimulation causes a large cranial displacement of the ribs and the sternum that leads to an expansion of the rib cage, particularly along its dorsoventral diameter, and to an increase in lung volume (46). Similarly, contraction of the sternomastoids in humans with transection of the upper cervical cord (such subjects have complete paralysis of the

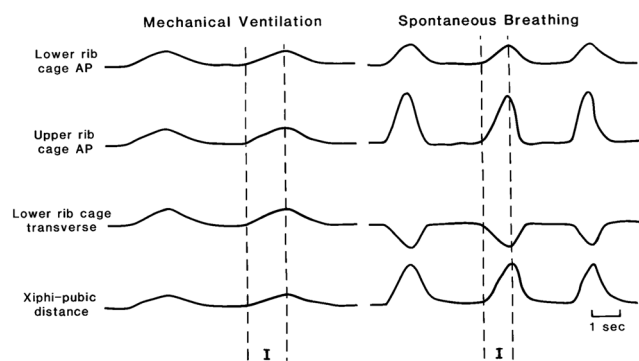


**Figure 16** Pattern of rib cage motion during mechanical ventilation (left) and during spontaneous breathing (right) in a quadriplegic subject with a traumatic transection of the upper cervical cord ( $C_1$ ). Each panel shows, from top to bottom, the respiratory changes in anteroposterior (AP) diameter of the lower rib cage, the changes in AP diameter of the upper rib cage, the changes in transverse diameter of the lower rib cage, and the changes in xiphi-pubic distance. Upward deflections correspond to an increase in diameter or an increase in xiphi-pubic distance (i.e., a cranial displacement of the sternum); I indicates the duration of inspiration. All rib cage diameters and the xiphi-pubic distance increase in phase during mechanical inflation. When the sternomastoids contract forcefully during spontaneous inspiration, however, the xiphi-pubic distance and the upper rib cage AP diameter increase proportionately more than the lower rib cage AP diameter, and the lower rib cage transverse diameter then decreases. (Reproduced, with permission, from De Troyer A. Mechanics of the chest wall muscles. In: Miller AD, Bianchi AL, Bishop B, editors. *Neural control of the respiratory muscles*, CRC Press, Inc., 1996, pp. 59–73).

diaphragm, intercostal, abdominal, and scalene muscles, but the sternomastoids are spared and contract forcefully during spontaneous inspiration) is associated with a marked cranial displacement of the sternum and a large expansion of the upper portion of the rib cage (22, 41, 67). This prominent cranial displacement of the sternum, however, combined with the fall in  $P_{pl}$  and  $P_{ab}$  resulting from the rib cage expansion, induces a decrease in the transverse diameter of the lower rib cage (Fig. 16).

The scalenes and sternomastoids have traditionally been regarded as “accessory” muscles of inspiration, and indeed, in the hamster, the scalenes are silent during resting breathing and show inspiratory activity when ventilation is increased by  $CO_2$ -enriched gas mixtures or when the mechanical load imposed on the inspiratory rib cage muscles is increased by phrenic nerve section or elevated inspiratory airflow resistance (78). Also, both muscles in the dog are almost invariably silent during breathing (35, 143, 144), and the sternomastoids in humans contract only during strong inspiratory efforts (15, 30, 90, 140). However, the scalenes in humans are always active during inspiration, including when the increase in lung volume is very small (30, 38, 80, 140); these muscles, therefore, must contribute to the inspiratory expansion of the rib cage and the lung.

Although the relative contributions of the scalenes and inspiratory intercostals to this expansion remain uncertain, two observations indicate that in humans, contraction of the

scalenes may be a significant determinant of the rib cage displacement during resting breathing. First, the inspiratory inward displacement of the upper rib cage that is commonly seen in subjects with quadriplegia due to traumatic transection of the lower cervical cord is usually absent in subjects with transection at the  $C_7$  level or below (69). As the scalenes are innervated from the lower five cervical segments, the muscles in such subjects typically remain active during inspiration, and the anteroposterior diameter of the upper rib cage tends to remain constant or even to increase slightly during inspiration. Second, as pointed out in section *Interactive effects on the rib cage*, the sternum in seated normal humans moves in the cranial direction during resting inspiration, such that the entire rib cage is displaced nearly along its relaxation trajectory (39). In contrast, in the dog, the scalenes are not active and the sternum moves in the caudal direction during resting inspiration (45). This species difference suggests that the inspiratory contraction of the scalenes in humans helps expand the rib cage with reduced distortion, although the predominant effect of the external intercostals over the parasternal intercostals may also play a role.

### Respiratory effect of the neck muscles and interaction with the inspiratory intercostals

Using computed tomography, Legrand et al. (115) measured the fractional changes in length and the masses ( $[\Delta L/(L\Delta V)]_{Rel}$  and  $m$  in Eq. (1), respectively) of the scalenes and sternomastoids in normal humans, and these measurements, combined with EMG recordings from the muscles during maximal static inspiratory efforts and postural efforts (81), led to the conclusion that the maximal  $\Delta P_{ao}$  produced by the isolated sternomastoids was approximately  $-3.0$   $cmH_2O$ . The corresponding  $\Delta P_{ao}$  value for the scalenes was approximately  $-3.5$   $cmH_2O$ , so the total  $\Delta P_{ao}$  generated by a maximal, simultaneous contraction of the scalenes and sternomastoids would amount to approximately  $-6.5$   $cmH_2O$ . In other words, in humans, the maximal inspiratory effect of the neck muscles contracting together would be approximately 40% of the effect of the external intercostals in all interspaces ( $-15$   $cmH_2O$ ) but at least twice as large as the effect of the parasternal intercostals in all interspaces ( $-2$  or  $3$   $cmH_2O$ ).

In the dog, the  $\Delta P_{ao}$  values recorded during simultaneous contraction of the parasternal intercostals in one interspace and either the scalenes or the sternomastoids are nearly equal to the sum of the  $\Delta P_{ao}$  values recorded during their separate contractions (116). Thus, as is the case for the different inspiratory intercostals among themselves, it appears that the interaction between the canine neck muscles and inspiratory intercostals on the lung is essentially additive, and there is no reason to believe that the interaction between these muscles in humans would be fundamentally different from that in the dog. On this basis, one would therefore predict that a forceful, simultaneous contraction of all the rib cage inspiratory muscles in normal humans would result in a  $\Delta P_{ao}$  of

approximately  $-25$  cmH<sub>2</sub>O; this value is close to the average pressure measured during maximal static inspiratory efforts in subjects with complete, isolated diaphragmatic paralysis (20, 103).

## The Abdominal Muscles

### Functional anatomy

The abdominal muscles with a significant respiratory function in quadrupeds and in humans are the four muscles that make up the ventrolateral wall of the abdomen. The rectus abdominis is the most ventral of these muscles. It originates from the ventral aspect of the sternum and the fifth, sixth and seventh costal cartilages, and it runs caudally along the whole length of the abdominal wall to insert into the pubis. The muscle is enclosed in a sheath formed by the aponeuroses of the three muscles situated laterally. The most superficial of these is the external oblique, which originates by fleshy digitations from the external surface of the lower eight ribs, well above the costal margin, and radiates caudally to insert on the iliac crest, the inguinal ligament, and the linear alba. The internal oblique lies deep to the external oblique. Its fibers arise from the iliac crest and inguinal ligament and diverge rostrally to insert on the costal margin and an aponeurosis contributing to the rectus sheath. Finally, deep to the internal oblique, lies the transversus abdominis, which arises from the inner surface of the lower six ribs, from the lumbar fascia, from the iliac crest, and from the inguinal ligament, runs circumferentially around the abdominal visceral mass, and terminates ventrally in the rectus sheath. Thus the fibers of the internal oblique are oriented about perpendicular to those of the external oblique and at a  $45^\circ$  angle relative to those of the transversus abdominis. Such a superposition of three muscle layers with different fiber orientations confers to the lateral abdominal wall a greater stiffness than any single muscle would (92).

### Respiratory action of the abdominal muscles

These four muscles have important functions as flexors and rotators of the trunk, but as respiratory muscles, the primary action of the external oblique, internal oblique, and transversus abdominis is to pull the abdominal wall inward and to increase  $P_{ab}$ . In so doing, they induce a cranial displacement of the diaphragm into the thoracic cavity, which leads to a rise in  $P_{pl}$  and, if the airway is open, to a decrease in lung volume. The rectus abdominis should act similarly when the ventral abdominal wall has an outward convexity, but it would be expected that, when the abdomen has an inward convexity, isolated contraction of the muscle would pull the wall slightly outward.

When the rectus abdominis in the dog is selectively activated by electrical stimulation, however, the ribs and sternum are displaced in the caudal direction and the anteroposterior

and transverse diameters of the lower rib cage decrease (59). The muscle, therefore, causes a rise in  $P_{ab}$  and  $P_{pl}$  regardless of the shape of the abdominal wall. On the other hand, although the other abdominal muscles also insert on the pelvis and the ribs, isolated stimulation of the canine internal oblique and transversus abdominis produces little or no rib cage displacement, and isolated stimulation of the external oblique causes a cranial displacement of the ribs and sternum with an increase in the anteroposterior and transverse diameters of the lower rib cage (59). D'Angelo et al. (23, 25) confirmed that simultaneous activation of all abdominal muscles in dogs and rabbits with the airway open produces an expansion of the rib cage. However, when the same activation was induced after evisceration, so that the rise in  $P_{ab}$  and  $P_{pl}$  during contraction was abolished, the lower rib cage contracted and the upper rib cage dimensions remained nearly unchanged (25).

These observations highlight the dual action of the abdominal muscles on the rib cage. On the one hand, the force they apply at their insertions on the ribs and the sternum acts to deflate the rib cage. On the other hand, by forcing the diaphragm cranially and stretching it, the rise in  $P_{ab}$  produced by the muscles induces both an increase in size of the zone of apposition of the diaphragm to the rib cage (Fig. 1) and an increase in passive diaphragmatic tension. This passive tension acts to raise the lower ribs and to expand the lower rib cage in the same way as does an active diaphragmatic contraction ("insertional" force of the diaphragm). The rise in  $P_{pl}$  resulting from the cranial displacement of the diaphragm also tends to expand the portion of the rib cage apposed to the lung. It is worth noting, however, that an expansion of the rib cage during abdominal muscle contraction opposes the deflation of the lung and, in that sense, may be viewed as a pressure dissipation; when rib cage elastance in dogs is increased by clamping the ribs and sternum, activation of the transversus abdominis produces a larger rise in  $P_{pl}$  for a given  $\Delta P_{ab}$  (19).

Irrespective of the rib cage displacement that they produce during isolated contraction, the four abdominal muscles deflate the lung. Based on the orientation and insertions of their fibers, however, one would predict that among these muscles, the transversus abdominis would have the greatest expiratory mechanical advantage. In agreement with the prediction, measurements of abdominal muscle length in supine dogs have shown that, although all muscles lengthen during passive lung inflation, the transversus abdominis lengthens by 25% of  $L_{FRC}$  as lung volume is passively increased from FRC to TLC (108). In contrast, the internal oblique lengthens by 15% of  $L_{FRC}$ , and the rectus abdominis and external oblique lengthen by only 1% to 3% of  $L_{FRC}$ . Also measurements of blood flow to the abdominal muscles with radioactive microspheres have shown that in supine anesthetized dogs, flow to the transversus abdominis increases during hyperpnea induced by CO<sub>2</sub>-enriched gas mixtures, whereas flow to the rectus abdominis and external oblique remains unchanged (144). A number of electrical recordings from the abdominal muscles in anesthetized dogs and cats (5, 83, 108) and in

unanesthetized dogs (43, 109) have also shown that the transversus abdominis and internal oblique are commonly active during expiration, whereas the rectus abdominis and external oblique usually remain silent. Thus, as is the case for the internal interosseous intercostals, the topographic distribution of neural expiratory drive to the canine abdominal muscles mirrors the topographic distribution of expiratory mechanical advantage. The changes in abdominal muscle length in humans have not been evaluated, but electromyographic studies have shown that as in the dog, when ventilation in healthy individuals is increased by CO<sub>2</sub>-enriched gas mixtures, expiratory activity in the transversus abdominis and internal oblique occurs well before activity can be recorded from either the rectus or the external oblique (1, 40).

### Effect of lung inflation

D'Angelo et al. (23) also produced abdominal muscle stimulation in dogs and rabbits at different lung volumes. In both animals,  $\Delta P_{ab}$  in response to a given activation slightly increased as lung volume before stimulation was increased above FRC; a similar small increase in  $\Delta P_{ab}$  with increasing lung volume has been reported during magnetic or electrical stimulation of the abdominal muscles in humans (70, 101, 117).  $\Delta P_{ao}$  also increased with increasing lung volume, in particular as lung volume approached TLC. D'Angelo et al. (23) concluded, therefore, that lung inflation enhances the lung-deflating action of the abdominal muscles, and they attributed this effect to a combination of muscle lengthening and decrease in diaphragmatic elastance.

To be sure, as pointed out in the previous section, passive lung inflation produces lengthening of the abdominal muscles, especially the transversus abdominis and the internal oblique (108). Passive inflation, however, also causes shortening of the diaphragm and so induces a decrease in passive diaphragmatic tension, particularly when the subjects are in the supine posture. Therefore, the load imposed by the diaphragm on the abdominal muscles decreases as lung volume increases, so that the amount of abdominal muscle shortening in response to a given activation should be greater. As a result, the abdominal muscles might be only a little longer during contraction at high lung volumes than during contraction at FRC, and, hence, in agreement with the observation of D'Angelo et al. (23),  $\Delta P_{ab}$  would be only a little greater. On the other hand, the decrease in passive diaphragmatic tension that occurs with passive inflation also implies that the rise in  $P_{ab}$  developed by an abdominal muscle contraction is better transmitted through the diaphragm to the pleural cavity. The rise in  $P_{pl}$  produced by a given rise in  $P_{ab}$ , therefore, is greater.

### Effect of ascites

Accumulation of liquid in the peritoneal cavity causes lengthening of the abdominal muscles as does passive lung inflation. In contrast to lung inflation, however, liquid accumulation also

lengthens the diaphragm, leading to an increase in passive diaphragmatic tension and an increase in diaphragm elastance (104). In the presence of liquid, therefore, the load imposed on the abdominal muscles during contraction is greater, and the amount of muscle shortening is smaller. As a result, the muscles develop greater force and generate larger  $\Delta P_{ab}$ , but the greater elastance of the diaphragm impedes the pressure transmission from the abdominal to the pleural cavity. Indeed, when the internal oblique and transversus abdominis muscles in supine dogs were stimulated in the presence of increasing amounts of liquid in the peritoneal cavity, the  $\Delta P_{ab}$  occurring in response to a given stimulation gradually increased as the amount of liquid increased to 100 ml/kg of body weight, but  $\Delta P_{ao}$  progressively decreased (107).

When the amount of liquid increased further to 200 ml/kg of body weight, however, the length of the relaxed abdominal muscles increased further and muscle shortening during stimulation became very small, so that the muscles during contraction were much longer, and yet  $\Delta P_{ab}$  decreased and returned toward the value measured before any liquid was introduced (107). Measurements of the internal oblique muscle length indicated that with 200 ml/kg of liquid, in fact, the abdominal muscles were excessively lengthened, so that their active length was well beyond  $L_o$ . In other words, the muscles operated on the descending limb, rather than the ascending limb, of their active length-tension curve, so that the force developed in response to a given activation was smaller. In addition, ascites also causes an increase in the cross-sectional area of the abdomen. Consequently, there was also a large increase in the radius of curvature of the transversus abdominis and perhaps of the internal oblique as well, so that the  $\Delta P_{ab}$  associated with a given muscle tension was probably reduced (Laplace's law).

### Interaction between the abdominal muscles and the expiratory intercostals

The interaction between the abdominal muscles and the expiratory intercostals on the lung and chest wall was also examined in rabbits by D'Angelo et al. (24). Because the internal interosseous intercostals and the triangularis sterni cannot be activated in all interspaces simultaneously, the action of these muscles was evaluated by applying an external pressure of 40 to 50 cmH<sub>2</sub>O on the rib cage; the action of the abdominal muscles was assessed by both compression of the abdomen with a similar external pressure and electrical stimulation of the muscles. As discussed in section *Respiratory action of the abdominal muscles*, isolated compression of the abdomen or maximal electrical stimulation of the abdominal muscles caused a rise in  $P_{pl}$  and  $P_{ab}$  with an expansion of the rib cage and a decrease in lung volume corresponding to approximately 65% of the expiratory reserve volume (ERV). On the other hand, during isolated compression of the rib cage, the decrease in lung volume was approximately 75% of ERV, and the rise in  $P_{pl}$  caused a caudal displacement of the diaphragm

and a rise in  $P_{ab}$  leading to an expansion of the abdomen. It appears, therefore, that the interaction between the abdominal and expiratory intercostal muscles on the chest wall is similar to that between the diaphragm and the inspiratory intercostals. That is, isolated contraction of either set of expiratory muscles produces prominent distortion of the chest wall and increases the elastic work of breathing, and coordinated contraction of the two sets of muscles reduces distortion and work.

The observations reported by D'Angelo et al. (24) further indicate that the sum of the lung volume reductions caused by separate compression of the abdomen and rib cage is substantially greater than the decrease in lung volume produced by their simultaneous compression (i.e., ERV), which would suggest that the interaction between the two sets of muscles on the lung could be antagonistic. However, as these investigators pointed out, the lung deflation produced by simultaneous abdominal and rib cage compression was probably limited by the closure of airways, rather than by the mechanical properties of the chest wall. In fact, the lengths of the abdominal and expiratory intercostal muscles are interdependent. Because isolated contraction of the abdominal muscles causes expansion of the rib cage, it should induce lengthening of the expiratory intercostals. Conversely, isolated contraction of the expiratory intercostals, by causing expansion of the abdomen, should induce lengthening of the abdominal muscles. It would be expected, therefore, that the two sets of muscles would have a synergistic interaction on the lung, but this prediction has yet to be validated.

### Interaction between the abdominal muscles and the diaphragm

Normal humans maintain the abdominal muscles quiescent when breathing at rest in the supine posture, but most subjects develop abdominal muscle activity, particularly in the lower regions of the abdomen, when adopting the standing posture (16, 31, 77, 119, 155). This activity is typically tonic, unrelated to the phases of the breathing cycle, and studies in subjects with transection of the upper cervical cord and pacing of the phrenic nerves have provided evidence that this tonic abdominal contraction may assist the action of the diaphragm (22, 154). Thus, when the subjects were supine, the unassisted paced diaphragm was able to generate an adequate tidal volume, but when they were tilted head-up or moved to the seated posture, so that the weight of the abdominal content caused a prominent outward displacement of the abdominal wall and a marked increase in end-expiratory lung volume, the tidal volume produced by pacing decreased by 40% or more relative to the supine posture. The decrease in tidal volume was significantly reduced, however, when a pneumatic cuff was inflated around the abdomen so as to mimic the tonic abdominal muscle contraction and prevent protrusion of the abdominal wall.

The beneficial effect of the abdominal muscles on the lung-expanding action of the diaphragm may be the result

of two mechanisms working separately or in combination. First, as pointed out in section *Respiratory action of the diaphragm*, a tonic abdominal muscle contraction or a cuff placed around the abdomen increases the elastance of the abdomen and thereby enhances the insertional and appositional forces of the diaphragm on the lower ribs. Consequently, the inspiratory action of the diaphragm on the lower rib cage is increased. Second, by contracting throughout the breathing cycle, the abdominal muscles make the diaphragm longer at the onset of inspiration and prevent it from shortening excessively during inspiration. As a result, the diaphragm develops greater force and generates larger pressure in much the same way as it does during contraction at lower lung volumes. To be sure, because tonic abdominal muscle contraction causes an increase in abdominal elastance, the increase in diaphragmatic force should translate only in part into an increase in  $\Delta P_{pl}$  (i.e.,  $\Delta P_{ab}$  should also be greater).

When the pneumatic cuff was placed around the quadriplegic subjects in the supine posture, however, it also induced an increased inspiratory expansion of the lower rib cage, but the tidal volume produced by pacing decreased, rather than increased (154). This suggests that the beneficial effect of the abdominal muscles on the lung-expanding action of the diaphragm in the head-up posture is primarily related to the increased length of the diaphragm, rather than the increased expansion of the lower rib cage. The role of the lower rib cage expansion in determining the lung-expanding action of the diaphragm, in fact, remains to be assessed.

### Conclusions

Since the publication in the mid-1980s of the previous edition of the *APS Handbook of Physiology-The Respiratory System*, significant progress has been made in the assessment and understanding of the mechanics of the respiratory muscles. It has become clear in particular that the pressure-generating capacity of the diaphragm is primarily determined by the length of the diaphragmatic muscle fibers during contraction, and that the muscle fiber length is, in turn, determined by the level of activation and by the load imposed on the muscle by the lung and chest wall. Thus, when the lung is passively inflated, the pressure generated by the diaphragm in response to a given activation is decreased because the muscle during contraction is shorter and generates less force. Conversely, when the load imposed on the muscle is increased, for example by the introduction of liquid in the abdominal cavity, the capacity of the diaphragm to generate pressure is increased because the muscle during contraction is longer and develops greater force. At very high lung volumes or in the presence of large amounts of liquid in the abdomen, however, the pressure-generating capacity of the diaphragm may also be impaired by an increase in the muscle radius of curvature.

Another prominent development has been the demonstration that, although the diaphragm is the main inspiratory



muscle, expanding the chest wall during breathing is an integrated process that involves many muscles, in particular the external intercostals in the dorsal portion of the rostral interspaces and the intercartilaginous portion of the internal intercostals (the so-called parasternal intercostals). Both in the dog and in humans, these two sets of intercostal muscles have an inspiratory effect (i.e., they cause a fall in  $P_{pl}$  during isolated contraction), and they contract during the inspiratory phase of the breathing cycle. The scalenes also contract during inspiration in humans. Coordinated activity between the external intercostals, parasternal intercostals, and scalenes helps the diaphragm expand the chest wall along its relaxation trajectory. In addition, by contracting during inspiration, these muscles increase the load on the diaphragm. Consequently, they also reduce the shortening of the diaphragm and enhance its pressure-generating ability.

In contrast to the parasternal intercostals and the external intercostals in the dorsal portion of the rostral interspaces, the internal interosseous intercostals in the caudal interspaces and the triangularis sterni have an expiratory effect (i.e., they cause a rise in  $P_{pl}$  during isolated contraction) and are active during expiratory efforts. These two sets of muscles, therefore, have an expiratory function during breathing, and they act in concert with the abdominal muscles to deflate the chest wall and the lung. The mechanisms for the inspiratory effect of the external intercostals in the dorsal portion of the rostral interspaces and the parasternal intercostals, and those for the expiratory effect of the triangularis sterni are well understood; they relate both to the nonuniform coupling between the ribs and the lung and to the orientation of the muscle fibers, adjusted to the three-dimensional configuration of the rib cage. The mechanism for the large expiratory effect of the internal interosseous intercostals in the caudal interspaces, however, is still unclear.

One of the most intriguing aspects of these recent developments, however, has been the observation of a remarkable congruence between the topographic distribution of neural drive to the intercostal muscles and the topographic distribution of mechanical advantage among them. Thus, both in the external intercostals and the parasternal intercostals in the dog and in humans, neural drive during resting inspiration is greater in the muscle areas with the greatest inspiratory mechanical advantage than in the areas with a smaller inspiratory mechanical advantage, and the muscle areas with an inspiratory mechanical advantage below some threshold remain electrically silent. The internal interosseous intercostals and abdominal muscles in the dog show a similar relationship, so that the muscle areas with the greatest expiratory mechanical advantage receive the greatest neural drive during expiration. More recently, similar relationships have also been reported for the canine diaphragm (14, 96) and the scalene muscles in the rabbit (113). Therefore, it would be tempting to speculate that activation and mechanical advantage might be correlated in nonrespiratory systems as well, but this hypothesis remains to be tested. The mechanisms that establish such relationships,

whether these relationships may adapt to alterations in mechanical advantage, and whether they have beneficial effects to the work or the metabolic cost of breathing remain also uncertain.

## References

1. Abe T, Kusuhara N, Yoshimura N, Tomita T, Easton PA. Differential respiratory activity of four abdominal muscles in humans. *J Appl Physiol* 80: 1379-1389, 1996.
2. Agostoni E, Mognoni P, Torri G, Agostoni A. Static features of the passive rib cage and diaphragm-abdomen. *J Appl Physiol* 20: 1187-1193, 1965.
3. Bainton CR, Kirkwood PA, Sears TA. On the transmission of the stimulating effects of carbon dioxide to the muscles of respiration. *J Physiol* 280: 249-272, 1978.
4. Bellemare F, Bigland-Ritchie B, Woods JJ. Contractile properties of the human diaphragm in vivo. *J Appl Physiol* 61: 1153-1161, 1986.
5. Bolser DC, Reier PJ, Davenport PW. Responses of the anterolateral abdominal muscles during cough and expiratory threshold loading in the cat. *J Appl Physiol* 88: 1207-1214, 2000.
6. Boriek AM, Black B, Hubmayr R, Wilson TA. Length and curvature of the dog diaphragm. *J Appl Physiol* 101: 794-798, 2006.
7. Boriek AM, Hwang W, Trinh L, Rodarte JR. Shape and tension distribution of the active canine diaphragm. *Am J Physiol Regul Integr Comp Physiol* 288: R1021-R1027, 2005.
8. Boriek AM, Kelly NG, Rodarte JR, Wilson TA. Biaxial constitutive relations for the passive canine diaphragm. *J Appl Physiol* 89: 2187-2190, 2000.
9. Boriek AM, Liu S, Rodarte JR. Costal diaphragm curvature in the dog. *J Appl Physiol* 75: 527-533, 1993.
10. Boriek AM, Rodarte JR. Effects of transverse fiber stiffness and central tendon on displacement and shape of a simple diaphragm model. *J Appl Physiol* 82: 1626-1636, 1997.
11. Boriek AM, Rodarte JR, Margulies SS. Zone of apposition in the passive diaphragm of the dog. *J Appl Physiol* 81: 1929-1940, 1996.
12. Boriek AM, Rodarte JR, Wilson TA. Kinematics and mechanics of midcostal diaphragm of dog. *J Appl Physiol* 83: 1068-1075, 1997.
13. Botha GSM. The anatomy of phrenic nerve termination and the motor innervation of the diaphragm. *Thorax* 12: 50-56, 1957.
14. Brancatisano A, Amis TC, Tully A, Kelly WT, Engel LA. Regional distribution of blood flow within the diaphragm. *J Appl Physiol* 71: 583-589, 1991.
15. Campbell EJM. The role of the scalene and sternomastoid muscles in breathing in normal subjects. An electromyographic study. *J Anat* 89: 378-386, 1955.
16. Campbell EJM, Green JH. The behavior of the abdominal muscles and the intra-abdominal pressure during quiet breathing and increased pulmonary ventilation. A study in man. *J Physiol* 127: 423-426, 1955.
17. Cappello M, De Troyer A. Interaction between left and right intercostal muscles in airway pressure generation. *J Appl Physiol* 88: 817-820, 2000.
18. Cappello M, De Troyer A. On the respiratory function of the ribs. *J Appl Physiol* 92: 1642-1646, 2002.
19. Cappello M, De Troyer A. Role of rib cage elastance in the coupling between the abdominal muscles and the lung. *J Appl Physiol* 97: 85-90, 2004.
20. Celli BR, Rassulo J, Corral R. Ventilatory muscle dysfunction in patients with bilateral idiopathic diaphragmatic paralysis: Reversal by intermittent external negative pressure ventilation. *Am Rev Respir Dis* 136: 1276-1278, 1987.
21. Close RI. Dynamic properties of mammalian skeletal muscles. *Physiol Rev* 52: 129-197, 1972.
22. Danon J, Druz WS, Goldberg NB, Sharp JT. Function for the isolated paced diaphragm and the cervical accessory muscles in C1 quadriplegics. *Am Rev Respir Dis* 119: 909-919, 1979.
23. D'Angelo E, Prandi E, Bellemare F. Mechanics of the abdominal muscles in rabbits and dogs. *Respir Physiol* 97: 275-291, 1994.
24. D'Angelo E, Prandi E, D'Angelo E, Pecchiari M. Lung-deflating ability of rib cage and abdominal muscles in rabbits. *Respir Physiol Neurobiol* 135: 17-24, 2003.
25. D'Angelo E, Prandi E, Robatto F, Petitjean M, Bellemare F. Insertional action of the abdominal muscles in rabbits and dogs. *Respir Physiol* 104: 147-157, 1996.
26. D'Angelo E, Sant' Ambrogio G. Direct action of contracting diaphragm on the rib cage in rabbits and dogs. *J Appl Physiol* 36: 715-719, 1974a.

27. D'Angelo E, Sant'Ambrogio G, Agostoni E. Effect of diaphragm activity or paralysis on distribution of pleural pressure. *J Appl Physiol* 37: 311-315, 1974b.
28. Da Silva KMC, Sayers BMA, Sears TA, Stagg DT. The changes in configuration of the rib cage and abdomen during breathing in the anaesthetized cat. *J Physiol* 266: 499-521, 1977.
29. Decramer M, Jiang TX, Demedts M. Effects of acute hyperinflation on chest wall mechanics in dogs. *J Appl Physiol* 63: 1493-1498, 1987.
30. Delhez L. *Contribution électromyographique à l'étude de la mécanique et du contrôle nerveux des mouvements respiratoires de l'homme*. Belgium: Vaillant-Carmanne, Liège, 1974.
31. De Troyer A. Mechanical role of the abdominal muscles in relation to posture. *Respir Physiol* 53: 341-353, 1983.
32. De Troyer A. Mechanics of the chest wall muscles. In: Miller AD, Bianchi AL, Bishop BP, editors. *Neural control of the respiratory muscles*. CRC Press, Inc., 1996, pp. 59-73.
33. De Troyer A. Respiratory muscle function. In: Shoemaker WC, Ayres SM, Grenvik A, Holbrook PR, editors. *Textbook of Critical Care*. W.B. Saunders, 2000, pp. 1172-1184.
34. De Troyer A. Impact of diaphragmatic contraction on the stiffness of the canine mediastinum. *J Appl Physiol* 105: 887-893, 2008.
35. De Troyer A, Cappello M, Brichant JF. Do canine scalene and sternomastoid muscles play a role in breathing? *J Appl Physiol* 76: 242-252, 1994.
36. De Troyer A, Cappello M, Leduc D, Gevenois PA. Role of the mediastinum in the mechanics of the canine diaphragm. *J Appl Physiol* 109: 27-34, 2010.
37. De Troyer A, Cappello M, Meurant N, Scillia P. Synergism between the canine left and right hemidiaphragms. *J Appl Physiol* 94: 1757-1765, 2003.
38. De Troyer A, Estenne M. Coordination between rib cage muscles and diaphragm during quiet breathing in humans. *J Appl Physiol* 57: 899-906, 1984.
39. De Troyer A, Estenne M, Ninane V. Rib cage mechanics in simulated diaphragmatic paralysis. *Am Rev Respir Dis* 132: 793-799, 1985.
40. De Troyer A, Estenne M, Ninane V, Van Gansbeke D, Gorini M. Transversus abdominis muscle function in humans. *J Appl Physiol* 68: 1010-1016, 1990.
41. De Troyer A, Estenne M, Vincken W. Rib cage motion and muscle use in high tetraplegics. *Am Rev Respir Dis* 133: 1115-1119, 1986.
42. De Troyer A, Farkas GA. Inspiratory function of the levator costae and external intercostal muscles in the dog. *J Appl Physiol* 67: 2614-2621, 1989.
43. De Troyer A, Gilmartin JJ, Ninane V. Abdominal muscle use during breathing in unanesthetized dogs. *J Appl Physiol* 66: 20-27, 1989.
44. De Troyer A, Gorman R, Gandevia SG. Distribution of inspiratory drive to the external intercostal muscles in humans. *J Physiol* 546: 943-954, 2003.
45. De Troyer A, Kelly S. Chest wall mechanics in dogs with acute diaphragm paralysis. *J Appl Physiol* 53: 373-379, 1982.
46. De Troyer A, Kelly S. Action of neck accessory muscles on rib cage in dogs. *J Appl Physiol* 56: 326-332, 1984.
47. De Troyer A, Kirkwood PA, Wilson TA. Respiratory action of the intercostal muscles. *Physiol Rev* 85: 717-756, 2005.
48. De Troyer A, Leduc D. Effect of inflation on the coupling between the ribs and the lung in dogs. *J Physiol* 555: 481-488, 2004.
49. De Troyer A, Leduc D. Effect of diaphragmatic contraction on the action of the canine parasternal intercostals. *J Appl Physiol* 101: 169-175, 2006.
50. De Troyer A, Leduc D. Role of pleural pressure in the coupling between the intercostal muscles and the ribs. *J Appl Physiol* 102: 2332-2337, 2007.
51. De Troyer A, Leduc D, Cappello M, Mine B, Gevenois PA, Wilson TA. Mechanisms of the inspiratory action of the diaphragm during isolated contraction. *J Appl Physiol* 107: 1736-1742, 2009.
52. De Troyer A, Legrand A. Inhomogenous activation of the parasternal intercostals during breathing. *J Appl Physiol* 79: 55-62, 1995.
53. De Troyer A, Legrand A. Mechanical advantage of the canine triangularis sterni. *J Appl Physiol* 84: 562-568, 1998.
54. De Troyer A, Legrand A, Gevenois PA, Wilson TA. Mechanical advantage of the human parasternal intercostal and triangularis sterni muscles. *J Physiol* 513: 915-925, 1998.
55. De Troyer A, Legrand A, Wilson TA. Rostrocaudal gradient of mechanical advantage in the parasternal intercostal muscles of the dog. *J Physiol* 495: 239-246, 1996.
56. De Troyer A, Legrand A, Wilson TA. Respiratory mechanical advantage of the canine external and internal intercostal muscles. *J Physiol* 518: 283-289, 1999.
57. De Troyer A, Loring SH. Actions of the respiratory muscles. In: Rousos C, editor. *The Thorax* (2nd ed), Vol. 85. New York: Marcel Dekker, 1995, pp. 535-563.
58. De Troyer A, Ninane V. Triangularis sterni: A primary muscle of breathing in the dog. *J Appl Physiol* 60: 14-21, 1986.
59. De Troyer A, Sampson M, Sigrist S, Kelly S. How the abdominal muscles act on the rib cage. *J Appl Physiol* 54: 465-469, 1983.
60. De Troyer A, Sampson M, Sigrist S, Macklem PT. Action of costal and crural parts of the diaphragm on the rib cage in dog. *J Appl Physiol* 53: 30-39, 1982.
61. De Troyer A, Wilson TA. The canine parasternal and external intercostal muscles drive the ribs differently. *J Physiol* 523: 799-806, 2000.
62. De Troyer A, Wilson TA. Coupling between the ribs and the lung in dogs. *J Physiol* 540: 231-236, 2002.
63. De Troyer A, Wilson TA. Effect of acute inflation on the mechanics of the inspiratory muscles. *J Appl Physiol* 107: 315-323, 2009.
64. DiMarco AF, Romaniuk JR, Supinski GS. Mechanical action of the interosseous intercostal muscles as a function of lung volume. *Am Rev Respir Dis* 142: 1041-1046, 1990.
65. DiMarco AF, Romaniuk JR, Supinski GS. Parasternal and external intercostal responses to various respiratory maneuvers. *J Appl Physiol* 73: 979-986, 1992.
66. DiMarco AF, Supinski GS, Budzinska K. Inspiratory muscle interaction in the generation of changes in airway pressure. *J Appl Physiol* 66: 2573-2578, 1989.
67. Duchenne GB. *Physiologie des Mouvements*. Paris: Baillière, 1967.
68. Easton PA, Fitting JW, Arnoux R, Guerraty A, Grassino AE. Recovery of diaphragm function after laparotomy and chronic sonomicrometer implantation. *J Appl Physiol* 66: 613-621, 1989.
69. Estenne M, De Troyer A. Relationship between respiratory muscle electromyogram and rib cage motion in tetraplegia. *Am Rev Respir Dis* 132: 53-59, 1985.
70. Estenne M, Pinet C, De Troyer A. Abdominal muscle strength in patients with tetraplegia. *Am J Respir Crit Care Med* 161: 707-712, 2000.
71. Estenne M, Yernault JC, De Troyer A. Rib cage and diaphragm-abdomen compliance in humans: Effects of age and posture. *J Appl Physiol* 59: 1842-1848, 1985.
72. Evanich MJ, Franco MJ, Lourenco RV. Force output of the diaphragm as a function of phrenic nerve firing and lung volume. *J Appl Physiol* 35: 208-212, 1973.
73. Farkas GA. Mechanical properties of respiratory muscles in primates. *Respir Physiol* 86: 41-50, 1991.
74. Farkas GA, Decramer M, Rochester DF, De Troyer A. Contractile properties of intercostal muscles and their functional significance. *J Appl Physiol* 59: 528-535, 1985.
75. Farkas GA, Rochester DF. Functional characteristics of canine costal and crural diaphragm. *J Appl Physiol* 65: 2253-2260, 1988a.
76. Farkas GA, Rochester DF. Characteristics and functional significance of canine abdominal muscles. *J Appl Physiol* 65: 2427-2433, 1988b.
77. Floyd WF, Silver PHS. Electromyographic study of patterns of activity of the anterior abdominal wall muscles in man. *J Anat* 84: 132-145, 1950.
78. Fournier M, Lewis MI. Functional role and structure of the scalene: An accessory inspiratory muscle in hamster. *J Appl Physiol* 91: 2436-2444, 1996.
79. Gandevia SC, Hudson AL, Gorman RB, Butler JE, De Troyer A. Spatial distribution of inspiratory drive to the parasternal intercostal muscles in humans. *J Physiol* 573: 263-275, 2006.
80. Gandevia SC, Leeper JB, McKenzie DK, De Troyer A. Discharge frequencies of parasternal intercostal and scalene motor units during breathing in normal and COPD subjects. *Am J Respir Crit Care Med* 153: 622-628, 1996.
81. Gandevia SC, McKenzie DK, Plassman BL. Activation of human respiratory muscles during different voluntary manoeuvres. *J Physiol* 428: 387-403, 1990.
82. Gauthier AP, Verbanck S, Estenne M, Segebarth C, Macklem PT, Paiva M. Three-dimensional reconstruction of the in vivo human diaphragm shape at different lung volumes. *J Appl Physiol* 76: 495-506, 1994.
83. Gilmartin JJ, Ninane V, De Troyer A. Abdominal muscle use during breathing in the anesthetized dog. *Respir Physiol* 70: 159-171, 1987.
84. Greer JJ, Martin TP. Distribution of muscle fiber types and EMG activity in cat intercostal muscles. *J Appl Physiol* 69: 2050-2056, 1990.
85. Hamberger GE. *De Respirationis Mechanismo et usu Genuino*. Germany: Jena, 1749.
86. Hershenson MB, Kikuchi Y, Loring SH. Relative strengths of the chest wall muscles. *J Appl Physiol* 65: 852-862, 1988.
87. Higenbottam T, Allen D, Loh L, Clark TJH. Abdominal wall movement in normals and patients with hemidiaphragmatic and bilateral diaphragmatic palsy. *Thorax* 32: 589-595, 1977.
88. Hilaire GG, Nicholls JG, Sears TA. Central and proprioceptive influences on the activity of the levator costae motoneurons in the cat. *J Physiol* 342: 527-548, 1983.
89. Hubmayr RD, Sprung J, Nelson S. Determinants of transdiaphragmatic pressure in dogs. *J Appl Physiol* 69: 2050-2056, 1990.
90. Hudson AL, Gandevia SC, Butler JE. The effect of lung volume on the co-ordinated recruitment of scalene and sternomastoid muscles in humans. *J Physiol* 584: 261-270, 2007.

91. Hwang JC, Zhou D, St John WM. Characterization of expiratory intercostal activity to triangularis sterni in cats. *J Appl Physiol* 67: 1518-1524, 1989.
92. Hwang W, Carvalho JC, Tarlovsky I, Boriek AM. Passive mechanics of canine internal abdominal muscles. *J Appl Physiol* 98: 1829-1835, 2005.
93. Hwang W, Kelly NG, Boriek AM. Passive mechanics of muscle tendinous junction of canine diaphragm. *J Appl Physiol* 98: 1328-1333, 2005.
94. Jefferson NC, Ogawa T, Necheles H. Trophic effects in the absence of respiratory function of the phrenic nerve. *Am J Physiol* 193: 563-566, 1958.
95. Jiang TX, Deschepper K, Demedts M, Decramer M. Effects of acute hyperinflation on the mechanical effectiveness of the parasternal intercostals. *Am Rev Respir Dis* 139: 522-528, 1989.
96. Johnson RL Jr, Hsia CCW, Takeda SI, Wait JL, Glenny RW. Efficient design of the diaphragm: Distribution of blood flow relative to mechanical advantage. *J Appl Physiol* 93: 925-930, 2002.
97. Kim MJ, Druz WS, Danon J, Machnach W, Sharp JT. Mechanics of the canine diaphragm. *J Appl Physiol* 41: 369-382, 1976.
98. Kirkwood PA, Sears TA, Stagg D, Westgaard RH. The spatial distribution of synchronization of intercostal motoneurons in the cat. *J Physiol* 327: 137-155, 1982.
99. Konno K, Mead J. Measurement of the separate volume changes of rib cage and abdomen during breathing. *J Appl Physiol* 22: 407-422, 1967.
100. Kreitzer SM, Feldman NT, Saunders NA, Ingram RH Jr. Bilateral diaphragmatic paralysis with hypercapnic respiratory failure. *Am J Med* 65: 89-95, 1978.
101. Kyroussis D, Polkey MI, Mills GH, Hughes PD, Moxham J, Green M. Simulation of cough in man by magnetic stimulation of the thoracic nerve roots. *Am J Respir Crit Care Med* 158: 1696-1699, 1997.
102. Landau BR, Akert K, Roberts TS. Studies on the innervation of the diaphragm. *J Comp Neurol* 119: 1-10, 1962.
103. Laroche CM, Carroll M, Moxham J, Green M. Clinical significance of severe isolated diaphragm weakness. *Am Rev Respir Dis* 138: 862-866, 1988.
104. Leduc D, Cappello M, Geveno PA, De Troyer A. Mechanics of the canine diaphragm in ascites: A CT study. *J Appl Physiol* 104: 423-428, 2008.
105. Leduc D, De Troyer A. The effect of lung inflation on the inspiratory action of the canine parasternal intercostals. *J Appl Physiol* 100: 585-588, 2006.
106. Leduc D, De Troyer A. Dysfunction of the canine respiratory muscle pump in ascites. *J Appl Physiol* 102: 650-657, 2007.
107. Leduc D, De Troyer A. Impact of acute ascites on the action of the canine abdominal muscles. *J Appl Physiol* 104: 1568-1573, 2008.
108. Leevers AM, Road JD. Mechanical response to hyperinflation of the two abdominal muscle layers. *J Appl Physiol* 66: 2189-2195, 1989.
109. Leevers AM, Road JD. Abdominal muscle activity during hypercapnia in awake dogs. *J Appl Physiol* 77: 1393-1398, 1994.
110. Legrand A, Brancatisano A, Decramer M, De Troyer A. Rostrocaudal gradient of electrical activation in the parasternal intercostal muscles of the dog. *J Physiol* 495: 247-254, 1996.
111. Legrand A, De Troyer A. Spatial distribution of external and internal intercostal activity in dogs. *J Physiol* 518: 291-300, 1999.
112. Legrand A, Goldman S, Damhaut P, De Troyer A. Heterogeneity of metabolic activity in the canine parasternal intercostals during breathing. *J Appl Physiol* 90: 811-815, 2001.
113. Legrand A, Majcher M, Joly E, Bonaert A, Geveno PA. Neuromechanical matching of drive in the scalene muscle in the anesthetized rabbit. *J Appl Physiol* 107: 741-748, 2009.
114. Legrand A, Ninane V, De Troyer A. Mechanical advantage of sternomastoid and scalene muscles in dogs. *J Appl Physiol* 82: 1517-1522, 1997.
115. Legrand A, Schneider E, Geveno PA, De Troyer A. Respiratory effects of the scalene and sternomastoid muscles in humans. *J Appl Physiol* 94: 1467-1472, 2003.
116. Legrand A, Wilson TA, De Troyer A. Rib cage muscle interaction in airway pressure generation. *J Appl Physiol* 85: 198-203, 1998.
117. Lim J, Gorman RB, Saboisky JP, Gandevia SC, Butler JE. Optimal electrode placement for noninvasive electrical stimulation of human abdominal muscles. *J Appl Physiol* 102: 1612-1617, 2007.
118. Loring SH. Action of human respiratory muscles inferred from finite element analysis of rib cage. *J Appl Physiol* 72: 1461-1465, 1992.
119. Loring SH, Mead J. Abdominal muscle use during quiet breathing and hyperpnea in uninformed subjects. *J Appl Physiol* 52: 700-704, 1982a.
120. Loring SH, Mead J. Action of the diaphragm on the rib cage inferred from a force-balance analysis. *J Appl Physiol* 53: 756-760, 1982b.
121. Loring SH, Woodbridge JA. Intercostal muscle action inferred from finite-element analysis. *J Appl Physiol* 70: 2712-2718, 1991.
122. Margulies SS, Farkas GA, Rodarte JR. Effects of body position and lung volume on in situ operating length of canine diaphragm. *J Appl Physiol* 69: 1702-1708, 1990.
123. Margulies SS, Rodarte JR, Hoffman EA. Geometry and kinematics of dog ribs. *J Appl Physiol* 67: 707-712, 1989.
124. Marshall R. Relationships between stimulus and work of breathing at different lung volumes. *J Appl Physiol* 17: 917-921, 1962.
125. McCool FD, Loring SH, Mead J. Rib cage distortion during voluntary and involuntary breathing acts. *J Appl Physiol* 58: 1703-1712, 1985.
126. McCully DK, Faulkner JA. Length-tension relationship of mammalian diaphragm muscles. *J Appl Physiol* 54: 1681-1686, 1983.
127. McKenzie DK, Gorman RB, Tolman J, Pride NB, Gandevia SC. Estimation of diaphragm length in patients with severe chronic obstructive pulmonary disease. *Respir Physiol* 123: 225-234, 2000.
128. Mead J. Mechanics of the chest wall. In: Pengelly LD, Rebuck AS, Campbell EJM, editors. *Loaded Breathing*. Edinburgh: Churchill Livingstone, 1974, pp. 35-49.
129. Mead J. Functional significance of the area of apposition of diaphragm to rib cage. *Am Rev Respir Dis* 119: 31-32, 1979.
130. Mead J, Loring SH. Analysis of volume displacement and length changes of the diaphragm during breathing. *J Appl Physiol* 53: 750-755, 1982.
131. Mead J, Yoshino K, Kikuchi Y, Barnas M, Loring SH. Abdominal pressure transmission in humans during slow breathing maneuvers. *J Appl Physiol* 68: 1850-1853, 1990.
132. Minh VD, Dolan GF, Konopka RF, Moser KM. Effect of hyperinflation on inspiratory function of the diaphragm. *J Appl Physiol* 40: 67-73, 1976.
133. Mortola JP, Sant' Ambrogio G. Motion of the rib cage and the abdomen in tetraplegic patients. *Clin Sci Mol Med* 54: 25-32, 1978.
134. Newman S, Road J, Bellemare F, Clozel JP, Lavigne CM, Grassino A. Respiratory muscle length measured by sonomicrometry. *J Appl Physiol* 56: 753-764, 1984.
135. Newsom Davis J, Goldman M, Loh L, Casson M. Diaphragm function and alveolar hypoventilation. *Q J Med* 65: 87-100, 1976.
136. Ninane V, Gorini M. Adverse effect of hyperinflation on parasternal intercostals. *J Appl Physiol* 77: 2201-2206, 1994.
137. Pengelly LD, Alderson AM, Milic-Emili J. Mechanics of the diaphragm. *J Appl Physiol* 30: 797-805, 1971.
138. Petroll WM, Knight H, Rochester DF. Effect of lower rib cage expansion and diaphragm shortening on the zone of apposition. *J Appl Physiol* 68: 484-488, 1990.
139. Pettiaux N, Cassart M, Paiva M, Estenne M. Three-dimensional reconstruction of human diaphragm with the use of spiral computed tomography. *J Appl Physiol* 82: 998-1002, 1997.
140. Raper AJ, Thompson WT Jr, Shapiro W, Patterson JL Jr. Scalene and sternomastoid muscle function. *J Appl Physiol* 21: 497-502, 1966.
141. Ringel ER, Loring SH, Mead J, Ingram RH Jr. Chest wall distortion during resistive inspiratory loading. *J Appl Physiol* 60: 63-70, 1986.
142. Road J, Newman S, Derenne JP, Grassino A. In vivo length-force relationship of canine diaphragm. *J Appl Physiol* 60: 63-70, 1986.
143. Robertson CH Jr, Foster GH, Johnson RL Jr. The relationship of respiratory failure to the oxygen consumption of, lactate production by, and distribution of blood flow among respiratory muscles during increasing inspiratory resistance. *J Clin Invest* 59: 31-42, 1977.
144. Robertson CH Jr, Pagel MA, Johnson RL Jr. The distribution of blood flow, oxygen consumption, and work output among the respiratory muscles during unobstructed hyperventilation. *J Clin Invest* 59: 43-50, 1977.
145. Rosenblueth A, Alanis J, Pilar G. The accessory motor innervation of the diaphragm. *Arch Int Physiol Biochim* 69: 19-25, 1961.
146. Sant' Ambrogio G, Saibene F. Contractile properties of the diaphragm in some mammals. *Respir Physiol* 10: 349-357, 1970.
147. Saumarez RC. An analysis of action of intercostal muscles in human upper rib cage. *J Appl Physiol* 60: 690-701, 1986.
148. Sears TA. Efferent discharges in alpha and fusimotor fibres of intercostal nerves of the cat. *J Physiol* 174: 295-315, 1964.
149. Sharp JT, Goldberg NB, Druz WS, Danon J. Relative contributions of rib cage and abdomen to breathing in normal subjects. *J Appl Physiol* 39: 608-618, 1975.
150. Smith J, Bellemare F. Effect of lung volume on in vivo contraction characteristics of human diaphragm. *J Appl Physiol* 62: 1893-1900, 1987.
151. Sprung J, Deschamps C, Hubmayr RD, Walters BJ, Rodarte JR. In vivo regional diaphragm function in dogs. *J Appl Physiol* 67: 655-662, 1989.
152. Sprung J, Deschamps C, Margulies SS, Hubmayr RD, Rodarte JR. Effect of body position on regional diaphragm function in dogs. *J Appl Physiol* 69: 2296-2302, 1990.
153. Strauss LH. *Z Ges Exptl Med* 86: 244, 1933, cited by Leigh Collins J, Satchwell LM, Abrams LD. Nerve supply to the crura of the diaphragm. *Thorax* 9: 22-25, 1954.
154. Strohl KP, Mead J, Banzett RB, Lehr J, Loring SH, O'Cain CF. Effect of posture on upper and lower rib cage motion and tidal volume during diaphragm pacing. *Am Rev Respir Dis* 130: 320-321, 1984.

155. Strohl KP, Mead J, Banzett RB, Loring SH, Kosch P. Regional differences in abdominal muscle activity during various maneuvers in humans. *J Appl Physiol* 51: 1471-1476, 1981.
156. Taylor A. The contribution of the intercostal muscles to the effort of respiration in man. *J Physiol* 151: 390-402, 1960.
157. Urmey WF, De Troyer A, Kelly SB, Loring SH. Pleural pressure increases during inspiration in the zone of apposition of diaphragm to rib cage. *J Appl Physiol* 65: 2207-2212, 1988.
158. Wilson TA, Boriek AM, Rodarte JR. Mechanical advantage of the canine diaphragm. *J Appl Physiol* 85: 2284-2290, 1998.
159. Wilson TA, De Troyer A. Effect of respiratory muscle tension on lung volume. *J Appl Physiol* 73: 2283-2288, 1992.
160. Wilson TA, De Troyer A. Respiratory effect of the intercostal muscles in the dog. *J Appl Physiol* 75: 2636-2645, 1993.
161. Wilson TA, De Troyer A. The two mechanisms of intercostal muscle action on the lung. *J Appl Physiol* 96: 483-488, 2004.
162. Wilson TA, De Troyer A. Diagrammatic analysis of the respiratory action of the diaphragm. *J Appl Physiol* 108: 251-255, 2010.
163. Wilson TA, Legrand A, Gevenois PA, De Troyer A. Respiratory effects of the external and internal intercostal muscles in humans. *J Physiol* 530: 319-330, 2001.